

The contamination of the surface of Vesta by impacts and the delivery of the dark material

D. Turrini^a, J.-P. Combe^b, T. B. McCord^b, N. Oklay^c, J.-B. Vincent^c, T. H. Prettyman^d, H. Y. McSween^e, G. J. Consolmagno SJ^f, M. C. De Sanctis^a, L. Le Corre^d, A. Longobardo^a, E. Palomba^a, C. T. Russell^g

^a*Istituto di Astrofisica e Planetologia Spaziali INAF-IAPS, Via del Fosso del Cavaliere 100, 00133, Rome, Italy.*

^b*Bear Fight Institute, 22 Fiddler's Road, Box 667, Winthrop, Washington 98862, USA.*

^c*Max Planck Institute for Solar System Research (MPS), Katlenburg-Lindau, Germany.*

^d*Planetary Science Institute, Tucson, Arizona 85719, USA.*

^e*University of Tennessee, Knoxville, Tennessee 37996, USA.*

^f*Specola Vaticana, V-00120, Vatican City State.*

^g*University of California, Los Angeles, California 90095, USA.*

Abstract

The Dawn spacecraft recently observed the presence of dark material, which in turn proved to be associated with the presence of OH and H-rich material, on the surface of Vesta. The source of this dark material has been almost unanimously identified with the low albedo asteroids, likely analogous to the carbonaceous chondrites found on Earth, that impacted on Vesta over its lifetime. However, it is still a matter of debate whether the delivery of the dark material is associated with a few large impact events, to micrometeorites or to the continuous, secular flux of impactors on Vesta. The “continuous flux” scenario, in particular, predicts that a significant fraction of the exogenous material accreted by Vesta should be due to non-dark impactors likely analogous to ordinary chondrites, which instead represent only a minor contaminant in the Howardite-Eucrite-Diogenite meteorites. In this work, we explored the “continuous flux” scenario and its implications for the composition of the vestan regolith, taking advantage of the data from the Dawn mission and the Howardite-Eucrite-Diogenite meteorites to constrain the contamination history of Vesta. We developed a model for the delivery of the exogenous material to Vesta and verified how the results it supplies are sensitive to the different parameters we consider. We calibrated the flux of impactors predicted by our model with the number of dark craters observed inside the Rheasilvia basin and we tested the assumptions on the impact conditions by studying the formation of Cornelia crater and of its dark deposits with a hydrocode simulation. We used our calibrated model to show that the “stochastic events” scenario and the “micrometeoritic flux” scenario are just natural consequences of the “continuous flux” scenario. We then used the model to estimate the amounts of dark and hydroxylate materials that were delivered on Vesta since the Late Heavy Bombardment and we showed how our results match well with the values estimated by the Dawn mission. We finally used our model to assess the amount of Fe and siderophile elements that the continuous flux of impactors would mix in the vestan regolith: concerning the siderophile elements, we focused our attention on the role of Ni. The results we obtained are in agreement with the data available on the Fe and Ni content of the Howardite-Eucrite-Diogenite meteorites and can be used as a reference frame in future studies of the data from the Dawn mission and of the Howardite-Eucrite-Diogenite meteorites. Our model cannot yet provide an answer to the conundrum of the fate of the missing non-carbonaceous contaminants, but we discuss some possible reasons for this discrepancy with the otherwise coherent picture described by our results.

Keywords: Asteroid Vesta, Impact processes, Asteroids, surfaces, Regoliths, Meteorites

Preprint submitted to Icarus

May 18, 2022

1. Introduction

The Dawn spacecraft recently observed the presence of dark material on the surface of Vesta (McCord et al., 2012; Reddy et al., 2012) and the dark material proved, in turn, to be associated with H-rich material (Prettyman et al., 2012) and OH (De Sanctis et al., 2012a). While the source of this dark material has been almost unanimously identified with the carbonaceous chondrites, particularly the CM and CR chondrites that have been observed as clasts inside the Howardite-Eucrite-Diogenite (HED) family of meteorites (see McCord et al. 2012; Reddy et al. 2012; Prettyman et al. 2012; De Sanctis et al. 2012a for more in-depth discussions), the actual delivery scenario is still debated.

McCord et al. (2012) linked the delivery of the dark material to the flux of low albedo impactors associated with the collisional history of Vesta since the Late Heavy Bombardment. Reddy et al. (2012) also associated the delivery of the dark material to impacting asteroids: however, instead of a continuous flux, these authors proposed that the delivery could be due to a few large, low-velocity impact events (at least two), one of these being responsible for the formation of the Veneneia basin. As an alternative possibility, Reddy et al. (2012) proposed that the dark material could be delivered by micrometeorites. As these authors pointed out, however, the micrometeoritic flux since the Late Heavy Bombardment is too low to account for the observed amount of dark material on Vesta. As the flux of dark micrometeorites was likely orders of magnitude more intense during the Late Heavy Bombardment, Reddy et al. (2012) suggested that the ancient meteoritic flux could have significantly contributed to the total budget of the dark material together with the impacts of low albedo asteroids.

In discussing the detection of OH in the spectral features of Vesta, De Sanctis et al. (2012a) linked its presence in the vestan regolith either to low-velocity impactors or to the micrometeoritic flux. These authors argued against a more or less continuous flux of OH-carrying impactors and favoured instead a temporally limited delivery,

possibly located in the more ancient past of Vesta (De Sanctis et al., 2012a). In discussing the distribution and setting of H-rich materials and studies of carbonaceous chondrite clasts in howardites, Prettyman et al. (2012) pointed out instead that the H content in the vestan regolith plausibly rules out a single, isolated impact or a temporally limited enhancement of the meteoritic flux as possible sources. These authors argued that the concentration and distribution of H suggests on the contrary an accumulation over time from numerous impactors and asteroidal dust (Prettyman et al., 2012).

In this work we will focus on the role of asteroidal impacts on Vesta in delivering the dark material, and the OH and H-rich material detected by the Dawn spacecraft. The “stochastic events” and the “micrometeoritic flux” scenarios discussed by Reddy et al. (2012) and De Sanctis et al. (2012a) are not necessarily in contrast with the “continuous flux” scenario discussed by McCord et al. (2012). As already noted by McCord et al. (2012), in the case of a continuous flux of impactors about half of the dark material would be delivered by a handful of large asteroids and an even larger contribution would be associated with stochastic events like the one responsible for Veneneia basin. Moreover, the “continuous flux” scenario naturally incorporates the “micrometeoritic flux” scenario. The “continuous flux” scenario, however, predicts that the dominant fraction of the exogenous material accreted by Vesta would be due to non-dark impactors (see e.g. McCord et al. 2012), likely analogous to ordinary chondrites. These contaminants have been detected only in marginal quantities in the HED family of meteorites (Lorenz et al., 2007), raising the conundrum of their fate.

The aim of this work is to address the problem of the contamination history of Vesta by providing a quantitative assessment of the amounts of the different exogenous materials delivered in the “continuous flux” scenario. To achieve this goal, we improved the model we first used in McCord et al. (2012) and refined the calculations performed there to estimate the flux of impactors and the amount of dark material delivered on Vesta

since the Late Heavy Bombardment. We tested the assumptions on the average impact velocity and angle by studying the formation of Cornelia crater with a hydrocode simulation and verifying that the distribution of the dark material inside the crater is satisfactorily reproduced by the remnants of the impactor material in the simulation. We extended our physical model to allow the assessment of the amounts of OH and H-rich material and of non-dark exogenous material delivered to Vesta. Concerning the latter class of contaminants, we focused on the role of Fe and of Ni, which we used as our tracer for the siderophile elements based on the results of Warren et al. (2009). We finally compared our results with the findings of the Dawn mission (De Sanctis et al., 2012a,b; McCord et al., 2012; Prettyman et al., 2012; Reddy et al., 2012; Yamashita et al., 2013) and discussed their implications for the composition of the vestan regolith in light of our current understanding of the HED family of meteorites (e.g. Zolensky et al. 1996; Lorenz et al. 2007; Warren et al. 2009).

2. Method

As we mentioned previously, our delivery scenario is based on the one we first employed in McCord et al. (2012). As such, it uses the intrinsic impact probability of Vesta together with a description of the temporal evolution of the population of the asteroid belt to statistically assess the number and sizes of the impactors on the asteroid. Using these values together with scaling laws for the retention efficiency of Vesta, it is then possible to estimate the amount of exogenous material accreted by the asteroid.

Following McCord et al. (2012), we used our current understanding of the present-day fraction of dark and non-dark asteroids to constrain the amount of potential carriers of dark material among the projectiles hitting Vesta. However, with respect to McCord et al. (2012) we also used the available information on the composition of the different classes of meteorites to try to quantitatively assess the amounts of the different materials delivered to the asteroid that

D_i (in km)	N_i
0.98	394278.90
1.23	296503.10
1.55	221080.10
1.96	162026.40
2.46	115400.30
3.10	78939.80
3.91	51398.50
4.92	31739.60
6.19	18630.70
7.79	10463.90
9.81	5671.80
12.40	2992.30
15.60	1548.00
19.60	789.70
24.60	554.00
31.00	338.00
39.10	224.00
49.20	185.00
61.90	164.00
77.90	116.00
98.10	91.00
123.50	64.00
155.50	38.00
195.70	17.00
246.40	8.00
≥ 300.00	6.00

Table 1: Present-day population of the asteroid belt. Column 1 is the central diameter estimated by Bottke et al. (2005a) for each bin from the magnitudes reported by Jedicke et al. (2002), while column 2 is the incremental number of asteroids in each bin from Jedicke et al. (2002). The total population of asteroids larger than ~ 1 km is therefore estimated to be $N_{belt} \approx 1.39 \times 10^6$. Table adapted from Bottke et al. (2005a). Note that, differently from Bottke et al. (2005a), the bins associated with diameters larger than ~ 300 km have been grouped into a single class as their populations are dominated by small number statistics.

could be measured by the Dawn mission.

In the following sections we will describe in detail all the aspects of our model. Before proceeding, we must point out that some of the observational parameters and of the theoretical results we used to build our model are still poorly constrained. As a consequence, in the model we considered different possibilities for these parameters in order to assess how much our results are affected by these uncertainties.

2.1. Temporal evolution of the asteroid population and flux of impactors on Vesta

In their work, McCord et al. (2012) analytically estimated the flux of dark impactors on Vesta based on the present day population of bodies with $D \geq 1$ km in the asteroid belt (see Table 1 and Bottke et al. 2005a).

The authors took into account the depletion in the population of asteroids that should have occurred across the last 3.5 Ga due to chaotic diffusion (estimated to be of a factor 2, Minton and Malhotra 2010) by assuming a constant decay (i.e. a linear decrease) in the number of asteroids over time. From the point of view of the total number of impacts (but not from that of their temporal distribution), this is equivalent to assuming a population constant in time that is 1.5 times larger than the present one. Using this approximation, McCord et al. (2012) estimated the flux of impactors on Vesta over the last 3.5 Ga by multiplying the number of impacts per unit time F_i for the integration time.

Following O’Brien and Sykes (2011), if we consider N_i impactors of diameter D_i (see Table 1) the impact frequency is $F_i = P_V A_i N_i$, where $P_V = 2.72 \times 10^{-18} \text{ km}^{-2} \text{ yr}^{-1}$ is the intrinsic impact probability of Vesta (O’Brien and Sykes, 2011), $A_i = (R_V + 0.5D_i)^2$ is the cross-sectional area of Vesta and the impactors (the factor π is included into P_V , Bottke et al. 1994) and $R_V = 262.7 \text{ km}$ is the mean radius of Vesta (Russell et al., 2012).

As a consequence, McCord et al. (2012) estimated the number of impacts n_i due to N_i impactors of a given size as

$$n_i = 1.5 F_i \Delta T = 1.5 P_V A_i N_i \Delta T \quad (1)$$

where $\Delta T = 3.5 \times 10^9$ years and the factor 1.5 is included to take into account the depletion of the asteroid belt, as discussed above.

In this work, we adopted a different approach, which more correctly accounts for the temporal evolution of the population of asteroids over time. Instead of considering the population as constant, we took advantage of the exponential decay law $f_t = C(t/1 \text{ year})^{-D}$ derived by Minton and Malhotra (2010), where f_t is the fraction of surviving bodies after the time t expressed in years while $C = 1.9556$ and $D = 0.0834$ are constants¹. Note that this equation or, more properly, these coefficients are valid (i.e. they reproduce the depletion rate of the asteroid belt) for $1 \text{ Ma} < t < 3.98 \text{ Ga}$ (Minton and Malhotra, 2010). Under these constraints, the value of f varies between 0.618 ($t = 1 \text{ Ma}$) and 0.309 ($t = 3.98 \text{ Ga}$, i.e. now).

Using these values and the present-day population of asteroids N_i from Table 1, we can extrapolate a primordial population of asteroids N_{ip} so that at each given time t we have $N_{it} = f_t N_{ip}$. This approach is made possible by the results of Bottke et al. (2005a,b), who showed that the present SFD of the asteroid belt should be stable over the temporal intervals we are considering. Note that, as in McCord et al. (2012), in this work we also focused our attention on the asteroids with estimated diameter $D \gtrsim 1 \text{ km}$, as shown in Table 1. The reasons for this choice is threefold.

First, we chose to base our model on the catalogued asteroid population and on the data from the Sloan Digital Sky Survey (SDSS) as reported by Jedicke et al. (2002). Therefore, while we take advantage of the magnitude to diameter conversion made by Bottke et al. (2005a), we are restricting ourselves only to the observational data and we are not including the results of modelling efforts (see e.g. Bottke et al. 2005b).

Second, the number of sub-km asteroids is still poorly constrained. Gladman et al. (2009) report

¹According to Minton and Malhotra (2010), the piecewise logarithmic law they derived is more accurate than the power law here used. The coefficients reported in their paper for the logarithmic law, however, appear to be incorrect and do not provide the correct depletion factor.

that the differential slope of the smaller asteroids, as estimated through the Sub-Kilometer Asteroid Diameter Survey (SKADS), is possibly steeper than previously thought (see also O’Brien and Sykes 2011). Specifically, Gladman et al. (2009) suggest that this uncertainty in the differential slope could result in an uncertainty of a factor 2 – 3 in the real number of sub-km asteroids.

Third, notwithstanding this uncertainty Gladman et al. (2009) report that the differential slope should be of the order of -2.5 . Values of the differential slope higher than -3 imply that the population of asteroids does not increase fast enough, when moving toward smaller sizes, to compensate for the decrease in mass due to the lower diameters of the bodies (e.g. Davis et al. 1979). Consequently, the mass contribution of sub-km asteroids will be more limited than that of km-sized asteroids.

The number of impacts n_i due to an evolving population of N_{it} impactors of a given size can therefore be computed as

$$n_i = \int P_V A_i N_{ip} f_t dt$$

In this work, we evaluated the previous integral over the desired temporal interval ΔT as a sum over discrete timesteps $\Delta t = 1000$ years, so that the previous equation becomes

$$n_i = \sum_j P_V A_i N_{ip} f_t(t_0 + j\Delta t) \quad (2)$$

where $t_0 = 1$ Ma and $0 \leq j \leq \Delta T/\Delta t$.

In the following, we will consider two temporal intervals ΔT : the post-Late Heavy Bombardment period or, more properly, the last 3.98 Ga, and the post-Rheasilvia period, i.e. the last 1 Ga (Schenk et al., 2012; Marchi et al., 2012). This choice is motivated by the following reasons.

First, following the time the average impact velocity on Vesta reached its present value, impacts removed from the asteroid several times more material than they brought (see e.g. Svetsov 2011). Turrini (2013), based on the results of McCord et al. (2012) and of S. Pirani (Master Thesis at the University of Rome “La Sapienza”), pointed

out that the combined effects of the impacts on Vesta during the Late Heavy Bombardment (as estimated in the scenario discussed by Minton and Malhotra 2009) and during the following 4 Ga could saturate the surface of the asteroid to a level equal to or slightly larger than the one currently observed in the oldest terrain ($\sim 10\%$, Marchi et al. 2012). In this case, most exogenous material deposited before the Late Heavy Bombardment could have been removed by later impacts.

Second, the collisional evolution of Vesta and, in general, of the asteroid belt before ~ 4 Ga ago is still debated. O’Brien et al. (2007) showed that the dynamical friction between planetesimals and planetary embryos could result in a depletion rate of the asteroid belt lower than that considered in the calculations of Bottke et al. (2005b), to now the most complete model of the collisional evolution of the asteroid belt. Also, the implications of the Late Heavy Bombardment in the framework of the updated, self-consistent version of the Nice Model (Levison et al., 2011) and those of a possible now-extinct extended population of the asteroid belt (Bottke et al., 2012) for the collisional history of Vesta have not been assessed to date. Dedicated studies would therefore be required before it is possible to reliably extend the model to earlier times.

Finally, the delivery of the exogenous material to Vesta at the time of the formation of its crust represents a separate chapter. Vesta (Turrini et al., 2011; Turrini, 2013) and, more generally, the asteroid belt (Turrini et al., 2012) underwent a phase of enhanced collisional evolution at the time of the formation of Jupiter. Turrini et al. (2011) and Turrini (2013) showed that the mass flux on Vesta due to the impactors could be of the order of $\sim 10\%$ of the present mass of the asteroid. However, as discussed by Turrini (2013), at that time Vesta still possessed a limited solid crust overlying a mostly molten interior (see e.g. Formisano et al. 2013), so the fate of these contaminants is still to be assessed. Moreover, the collisional evolution of Vesta during the phase of depletion of the asteroid belt (see Coradini et al. 2011 and O’Brien and Sykes 2011 and reference therein) plausibly removed most if not all of the exogenous material

previously deposited on the surface.

These reasons are at the basis of our decision to focus on the post-Late Heavy Bombardment temporal interval, for which the collisional evolution of the asteroid belt is better constrained (see e.g. Coradini et al. 2011 and O’Brien and Sykes 2011 and references therein). As the Dawn mission provided a constraint on the age of the Rheasilvia basin (1 Ga, Schenk et al. 2012; Marchi et al. 2012) and the excavation of this basin most likely removed all previous exogenous contaminants (see Schenk et al. 2012, Jutzi et al. 2013 and Ivanov and Melosh 2013), thus providing us with a “clean slate” from the point of view of the contamination, we decided to consider the last 1 Ga as an additional case.

2.2. Characterization of the impacts and of the different kind of impactors

As we are interested in the global effects of the collisional history of Vesta for the contamination of its surface, in our model we assumed that all impacts take place at the average impact velocity $V_i = 4.75$ km/s estimated by O’Brien and Sykes (2011) and occur at 45° respect to the local normal to the surface of the asteroid (Melosh, 1989). For the impactors, we adopted average densities of 1400 kg/m^3 for dark asteroids (i.e. the average density of C type asteroids from Britt et al. 2002; Carry 2012), of 2700 kg/m^3 for non-dark asteroids (i.e. the average density of S type asteroids from Britt et al. 2002; Carry 2012) and of 2400 kg/m^3 when considering all possible impactors (based on our reference fraction of dark asteroids in the asteroid belt described in Sect. 2.4).

Note that these densities are significantly lower (a few 10%) than the bulk densities of carbonaceous and ordinary chondrites (Consolmagno et al., 2008; Macke et al., 2011). In particular, the density of dark impactors is $\sim 30\%$ lower than the average bulk density of the CM-CR-CI meteorites ($\sim 2100 - 2200 \text{ kg/m}^3$, see Macke et al. 2011 and Sect. 2.4) that are the potential carriers of water to Vesta, as we will discuss in Sect. 2.4. Nevertheless, the values we adopted will provide us with a conservative estimate of the amounts of

exogenous materials delivered to Vesta over the temporal intervals here considered.

2.3. Mass retention efficiency

In their work, McCord et al. (2012) evaluated the fraction of the mass of the impacting bodies that is retained by Vesta by using Eq. 8 (valid for impact velocities $V \leq 15$ km/s) from Svetsov (2011), i.e.

$$f_r = (0.14 + 0.003V) \ln v_{esc} + 0.9V^{-0.24} \quad (3)$$

where $v_{esc} = 0.37$ km/s is the escape velocity from Vesta (Turrini et al., 2011) and $V = 4.75$ km/s is the average impact velocity of the impactors (O’Brien and Sykes, 2011). McCord et al. (2012) estimated that about 46.6% of the impacting mass would be retained by Vesta ($f_r = 0.466$). Therefore, if m_i is the mass of the impacting body, the mass retained by Vesta is thus $m_r = f_r m_i = 0.466 m_i$. Note that integrating the retention efficiency over the range of possible impact velocities computed by O’Brien and Sykes (2011) gives similar results to using solely the average impact speed, the difference in the retention factor being of the order of 10%.

In studying the delivery of volatile material on the Moon by cometary and asteroidal impacts, Ong et al. (2010) estimated that, assuming a median impact velocity of 20 km/s and averaging over all possible impact velocities, about 16.5% of the mass of impacting asteroids would be retained by the Moon. It must be noted that the study of Ong et al. (2010) focused mainly on cometary impactors, for which they provided the retention efficiencies at different impact velocities, and considered also the contribution of the re-condensation of water vapors. For asteroidal impactors, they instead provided only the average value previously reported. As the behavior of cometary impactors and asteroidal impactors is not necessarily comparable and for Vesta it is unlikely that the re-condensation of vapors played a significant role in the contamination of the surface of the asteroid (see e.g. Turrini et al. 2011), we focused only on the single value of the average retention efficiency reported for asteroidal impactors. To estimate the difference between the results of Ong et al. (2010)

and those of Svetsov (2011), we computed the average retained mass fraction for the Moon using the scaling laws reported by Svetsov (2011). Following Ong et al. (2010), we used an escape velocity of 2.38 km/s and an average impact velocity of 20 km/s. The logarithmic interpolation of Eqs. 8 and 9 from Svetsov (2011) for the chosen impact velocity gives an average retained mass of 55.7%. Therefore, the scaling laws by Svetsov (2011) result in a retention efficiency about 3.4 times larger than the results of Ong et al. (2010).

Before proceeding, it must be stressed that linearly scaling Eq. 3 to the results of Ong et al. (2010) obtained for an average impact velocity of 20 km/s is not necessarily correct over the range of impact velocities characteristic on Vesta (1–10 km/s, O’Brien and Sykes 2011). However, as we are mainly interested in understanding how much the uncertainty on the retention scaling law can affect the results of the model, in the following we will also consider the following case:

$$\begin{aligned} f_r^* &= 0.296 f_r \\ &= 0.296 \times ((0.14 + 0.003V) \\ &\quad \times \ln v_{esc} + 0.9V^{-0.24}) \end{aligned} \quad (4)$$

Using the same escape velocity and average impact speed we used for Eq. 3, Eq. 4 gives a retention efficiency $f_r^* = 0.138$.

2.4. Dark impactors, OH and H-rich material

McCord et al. (2012) estimated the fraction of low albedo impactors on Vesta computing the ratio between asteroids with B, C, P and D spectral types and all spectroscopically classified asteroids from the JPL Small-Body Database Search Engine². The value they obtained was $F_d = 0.22$. An independent estimate performed by De Sanctis et al. (2012a) consistently gave $0.1 \leq F_d \leq 0.3$.

In this work, we used the catalogue of asteroids from the JPL Small-Body Database Search Engine to assess the fraction of low albedo impactors on Vesta in three different ways, i.e.: 1) using the same method as McCord et al. (2012); 2) using the same method as McCord et al. (2012)

but including only asteroids with C, D and P spectral types; 3) computing the fraction of asteroids with albedo lower than or equal to 0.05 among all asteroids for which a value of albedo has been estimated. Method 1 held the same value as that computed by McCord et al. (2012), $F_{d1} = 0.22$. Method 2 held a value of $F_{d2} = 0.18$. Method 3 held a value of $F_{d3} = 0.28$. The number of dark impactors of a given size D_i over a temporal interval ΔT on Vesta is then

$$n_i^{dark} = n_i \times F_d \quad (5)$$

where n_i is obtained through Eq. 2 and F_d is one of the three values previously discussed. The amount of dark material delivered by these impactors can instead be expressed as

$$m_i^{dark} = \left(\frac{\pi}{6} D_i^3 \rho \right) \times f_r \times n_i^{dark} \quad (6)$$

where f_r is obtained either through Eq. 3 or Eq. 4 and ρ is the average density of the dark impactors. In the following we will use the value derived by McCord et al. (2012) and through our method 1 as our reference value. We will use the results of methods 2 and 3 to discuss how the uncertainty on the abundance of dark asteroids in the asteroids belt affects the results of the model.

Coincident with that of the dark material, the Dawn mission reported the presence of OH (De Sanctis et al., 2012a) and H-rich material (Prettyman et al., 2012) on Vesta. The results of Prettyman et al. (2012) and De Sanctis et al. (2012a) indicated a clear correlation between the presence of dark material and that of OH and H-rich material. Both H and OH are likely present in the vestan regolith in the form of hydrated minerals and not as water. However, in meteoritics (see e.g. Robert 2003) and in nuclear spectroscopy (see e.g. Prettyman 2007) their presence is generally quantified in terms of the equivalent amount of water needed to reproduce the measurements. In the following, therefore, we will refer to these two (likely overlapping) classes of materials with the common term of “water-equivalent material.”

As discussed by McCord et al. (2012), the dark impactors are plausibly asteroids similar in composition to the carbonaceous chondrites. The

²http://ssd.jpl.nasa.gov/sbdb_query.cgi

most efficient carriers of water-equivalent material among the dark impactors should therefore be those bodies similar in composition to the CM, CR and CI carbonaceous chondrites (Jarosewich, 1990; Robert, 2003). In particular, CM chondrites and, to a smaller extent, CR chondrites represent the dominant components of carbonaceous chondritic clasts observed in HED meteorites (Zolensky et al., 1996; Lorenz et al., 2007). The CR/CM ratio in HED meteorites, moreover, is the same as the one observed among modern CM and CR falls on Earth (Zolensky et al., 1996). Therefore, in order to assess the amount of water-equivalent material that a continuous flux of impactors would bring on Vesta, we tried to estimate the frequency of CM-, CR- and CI-like projectiles among the dark impactors hitting the asteroid. Based on the observation by Zolensky et al. (1996) that the CR/CM ratios are similar among meteorite falls on Earth and HEDs meteorites, we used the fluxes of the falls for the different classes of carbonaceous chondrites on Earth as our planetary analogue. From the Meteoritical Bulletin³, as of May 2013, we note that CM chondrites represent 34% of the falls of carbonaceous chondrites, CR chondrites represent 6.8% and CI chondrites 11.4%. The fraction of the masses of these impactors that represent water-equivalent material can be assumed, on average, $R_w = 0.1$, i.e. 10 wt% (Jarosewich, 1990; Robert, 2003).

If, following Zolensky et al. (1996), we focus only on CM and CR chondrites, we obtain that a fraction $F_w^{CM+CR} = 0.41$ of the dark impactors on Vesta would bring water-equivalent material to the asteroid. This will be our standard case. Should we include also CI chondrites, i.e. we assume that our database of carbonaceous clasts in HED meteorites is not complete, the fraction of carriers of water-equivalent material would rise to $F_w^{CM+CR+CI} = 0.53$. We caution the readers, however, that while this is possibly the best approximation we can make to date, it is not necessarily a good or physically meaningful one. As an example, CI chondrites are very fragile and the bulk of them likely do not survive the pas-

sage through the Earth’s atmosphere, causing the underestimation of their contribution. Moreover, there is no guarantee that the modern flux of meteorites on Earth is a meaningful approximation of the secular flux in the asteroid belt over one or more Ga, as it can be significantly affected by temporally-limited events like the break-up of an asteroid.

In order to better constrain the implications of the uncertainty on the flux of carriers of water-equivalent material for our results, we considered also the water delivery efficiency discussed by Ong et al. (2010). In their work, these authors assumed that about one-third of impacting asteroids would be C-type (our dark impactors, i.e. $F_d = 0.33$) and that two-thirds of those impactors would contain water-equivalent material ($F_w = 0.67$). These authors assumed an average 10 wt% water content, i.e. the same value we adopted in the previous cases. As these authors point out, their assumptions result in water representing 2.2% of the total mass flux due to impacts. As a comparison, in our reference case we have $F_{d1} \times F_w^{CM+CR} \times R_w = 0.9\%$, i.e. our reference water delivery efficiency is 2.5 times smaller.

Using the value of R_w and one of the possible values of F_w previously discussed, the amount of water-equivalent material m_i^w delivered on Vesta by dark impactors of a given size D_i over a temporal interval ΔT is then

$$m_i^w = m_i^{dark} \times F_w \times R_w \quad (7)$$

where m_i^{dark} is obtained through Eq. 6.

2.5. Fe and siderophile elements

As the Gamma Ray and Neutron Detector (GRaND) on-board the Dawn spacecraft measured the global Fe content of minerals on the surface of Vesta (Prettyman et al., 2012; Yamashita et al., 2013), we used our model to assess what a continuous flux of impactors would imply from the point of view of the contamination of the vestan regolith by Fe and siderophile elements. Concerning the latter, we focused our analysis on the role of Ni, which has been suggested by Warren et al. (2009) to play an important role as tracer of the regolith’s maturity and enrichment.

³<http://www.lpi.usra.edu/meteor>

In contrast to the cases of the dark material and the water-equivalent material discussed in Sect. 2.4, the howarditic material composing most of the vestan regolith (De Sanctis et al., 2012b; Prettyman et al., 2012) would contain amounts of Fe and Ni, even if uncontaminated. The mean Fe contents for diogenites and basaltic eucrites are respectively 13 wt% and 14.7 wt% (Jarosewich 1990; Prettyman et al. 2012, Supplementary Material). A 2:1 eucrite-diogenite mixture, suggested to be the average compositional mixture of howardites (Warren et al., 2009), would have an average Fe content of 14.1 wt%, which is consistent with the mean Fe content of 13.8 wt% of howardites (Jarosewich 1990; Prettyman et al. 2012, Supplementary Material). In order to be able to compare our results with the measurements of GRaND, we will follow Yamashita et al. (2013) and assume that the native Fe content of the vestan regolith is 13.8 wt%.

The Ni content of the different materials composing the vestan crust spans a greater range of values than Fe. The Ni content of diogenites varies between 5 – 200 $\mu\text{g/g}$, i.e. $5 \times 10^{-4} - 0.02$ wt% (Warren et al., 2009). Monomict and cumulate eucrites have a lower Ni content, ranging between 0.1 – 10 $\mu\text{g/g}$ (Warren et al., 2009), i.e. $10^{-5} - 10^{-3}$ wt%. Polymict eucrites have a Ni content similar to that of diogenites, with one exceptional polymict eucrite sample as rich in Ni as ~ 1000 $\mu\text{g/g}$, i.e. 0.1 wt% (Warren et al., 2009). Howardites are characterized by a large variability in Ni content and overlap the range of diogenites and polymict eucrites. According to Warren et al. (2009), Ni content in howardites varies in the range 10 – 5000 $\mu\text{g/g}$, i.e. $10^{-3} - 0.5$ wt%. If we assume, based on the values reported by Warren et al. (2009), an average Ni content of 1 $\mu\text{g/g}$ for eucrites and 40 $\mu\text{g/g}$ for diogenites, the resulting 2:1 mixture will have a Ni content of ~ 14 $\mu\text{g/g}$. This is also the order of magnitude of the Ni content of the more Ni-poor samples of howardites analyzed by Warren et al. (2009) and will be used in the following as our native Ni content of the vestan crust.

Contrary to HED meteorites, the order of magnitude of the Fe and Ni contents of chon-

drites (both ordinary and carbonaceous) is much less variable. Based on the values reported by Jarosewich (1990), the average Fe and Ni contents of all (both dark and non-dark) impactors in our model can be assumed to be respectively 20 wt% (i.e. $F_{Fe} = 0.2$) and 1 wt% (i.e. $F_{Ni} = 0.01$). The amount of Fe delivered on Vesta by impactors of a given size D_i over a temporal interval ΔT can then be expressed as

$$m_i^{Fe} = \frac{m_i^{dark}}{F_d} \times F_{Fe} \quad (8)$$

where m_i^{dark} is obtained through Eq. 6 and is divided by the value F_d to obtain the total mass delivered by dark and non-dark impactors. A similar equation holds for the case of Ni.

2.6. Crater saturation and ejecta blanketing

The effects of crater saturation and of the blanketing due to crater ejecta are two important factors that must be considered in discussing the contamination of Vesta. The estimate of the extent of vestan surface affected by craters over a given timespan and of the level of crater saturation reached would allow to assess how long the dark material can survive on the surface of Vesta before being removed by the impacts of non-dark asteroids and whether we should expect to be able to link most dark material to specific cratering events or not. The assessment of the degree to which crater ejecta cover the surface of the asteroid, on the other hand, would supply information on how much of the dark material is going to be buried to depths that cannot be probed by the instruments on-board the Dawn spacecraft and how old the dark material on the surface can be.

Given that our model already computes the flux of impactors hitting Vesta over the desired timespan in order to estimate the degree of contamination produced, we complemented it with a collisional model similar to the one described in Turrini (2013), to estimate the craters produced by the impacts and the degree of saturation they cause. Moreover, we included in the model also an estimate of the ejecta blanketing associated with the craters and of the surface area affected by the fragments of the dark impactors along the line of

what we already did in McCord et al. (2012), as described in their Supplementary Information.

The diameter of the craters produced by the flux of impactors was estimated using the following scaling law for rocky targets by Holsapple and Housen (2007):

$$\frac{R_c}{r_i} = 0.93 \left(\frac{g r_i}{V^2} \right)^{-0.22} \left(\frac{\rho_i}{\rho_v} \right)^{0.31} + 0.93 \left(\frac{Y_v}{\rho_v V^2} \right)^{-0.275} \left(\frac{\rho_i}{\rho_v} \right)^{0.4} \quad (9)$$

where R_c is the final radius of the crater, r_i is the radius of the impactor, $g = 0.22 \text{ m s}^{-2}$ is the surface gravity of Vesta (Reddy et al., 2012), $V = 3.36 \text{ km/s}$ is the average vertical impact velocity (to take into account the fact that impacts are assumed to take place at 45° respect to the normal to the surface, see Sect. 2.2), $Y_v = 7.6 \text{ MPa}$ is the strength of the material composing the surface of Vesta (assumed to behave as soft rock, Holsapple 1993), ρ_i is the density of the impactor and $\rho_v = 3090 \text{ kg m}^{-3}$ is the density of the crust of Vesta (Russell et al., 2012, 2013).

Using the diameters of the craters estimated this way, we computed the associated R-value distribution. Following the Crater Analysis Techniques Working Group (1978), we assumed an initial crater diameter $D_1 = 1 \text{ km}$ and we considered bins where $D_{i+1} = \sqrt{2}D_i$. For each $[D_i, D_{i+1})$ bin we computed the number of craters N_i and the geometric mean diameter

$$\overline{D}_i = \left(\prod_{j=1}^{N_i} d_j \right)^{\frac{1}{N_i}}$$

where d_j are the diameters of the individual craters. Then the R-value associated with each bin is computed as

$$R_i = \frac{N_i \overline{D}^3}{S_v (D_{i+1} - D_i)} \quad (10)$$

In building the R-value distributions, we considered only those bins where the cumulative number of craters was greater than or equal to 1.

As we mentioned previously, using the diameters computed with Eq. 9, we also computed the

cumulative surface affected by ejecta blanketing and the darkened surface due to the fragments of the dark impactors. To compute the overall blanketed surface we followed Melosh (1989) and assumed that, on average, ejecta cover a surface with radius twice as large as that of the associated crater. The total blanketed surface A_B then becomes

$$A_B = \sum_i \pi (D_i^2 - (0.5D_i)^2) = \sum_i \frac{3\pi}{4} D_i^2 \quad (11)$$

where we summed over the craters produced by all impactors (as also dark impactors excavate ejecta that can cover previously deposited dark material) during the relevant temporal interval, and we subtracted the contribution of the craters themselves, as in principle they can expose previously buried dark material.

To compute the darkened surface, we followed instead McCord et al. (2012) and assumed that the fragments from the dark impactors would distribute inside the crater and inside a cone 30° wide and extending up to 4 times the radius of the crater downstream to the impact direction. As a consequence, the total darkened surface is

$$A_B = \sum_i \left(\frac{\pi}{4} D_i^2 + \frac{\pi}{48} ((4D_i)^2 - D_i^2) \right) = \sum_i \left(\frac{\pi}{4} D_i^2 + \frac{5\pi}{16} D_i^2 \right) = \sum_i \frac{9\pi}{16} D_i^2 \quad (12)$$

where we sum only over the craters produced by dark impactors.

2.7. Cratering erosion

The assessment of the mass loss of Vesta from the formation of its basaltic crust to now is important to understand the global picture of the erosion of the surface of the asteroid (see e.g. McSween et al. 2013 for a discussion concerning Rheasilvia and Turrini 2013 for a more general one) and can play a significant role in unveiling the history of the asteroid belt and the Solar System (Coradini et al., 2011; Turrini et al., 2011, 2012; Turrini, 2013).

Understanding the balance between mass gain and mass loss due to impacts is also fundamental to constrain how long the exogenous material

can survive on the surface of Vesta and how ancient the dark deposits and veneers observed by the Dawn mission are. As a consequence, we used our model to assess the mass loss due to the cumulative flux of impactors over the two temporal intervals considered in this work.

The constraints on the thickness of the vestan regolith are still limited and the available estimates range from about 100 m to about 1 km (Jaumann et al. 2012, see also their Supplementary Materials). Using Eq. 9 for the different size bins reported in Table 1 and multiplying the results for the average depth-to-diameter ratio (0.168) estimated for Vesta by Vincent et al. (2013), we can see that all but possibly the smaller impactors here considered would excavate significantly deeper than the regolith layer. As a consequence, in our model we used the scaling law for rock from Holsapple and Housen (2007) to estimate the mass loss of Vesta.

From this scaling law in the angle-averaged form computed by Svetsov (2011) we obtain

$$f_e = \frac{M_e}{m_i} = 0.03 \left(\frac{V}{v_{esc}} \right)^{1.65} \left(\frac{\rho_i}{\rho_V} \right)^{0.2} = 2.13 \quad (13)$$

where M_e is the eroded mass, m_i is the mass of the impactor, V is the average impact velocity (see Sect. 2.2), $v_{esc} = 0.37$ km/s is the escape velocity from Vesta (Turrini et al., 2011), $\rho_i = 2400$ kg/m³ is the average density assumed for all impactors (see Sect. 2.2) and $\rho_{reg} = 3090$ kg/m³ is the assumed density of the crust (regolith plus bedrock) of Vesta (Russell et al., 2012, 2013).

The total eroded mass due to impactors of a given size D_i over a temporal interval ΔT can then be expressed as

$$m_i^{erod.} = \left(\frac{\pi}{6} D_i^3 \rho_i \right) \times n_i \times f_e \quad (14)$$

where n_i is obtained from Eq. 2 and f_e is obtained from Eq. 13. We can already see, however, that cratering erosion will be between about 5 times (if Eq. 3 is used for the retention efficiency) and 15 times (if Eq. 4 is used instead) more efficient than mass accretion.

2.8. Hydrocode modeling and validation of the impact parameters

To verify whether the average impact velocity and impact angle we assumed for all impactors are appropriate choices to study the delivery of the dark material, we complemented our model with a hydrocode simulation devised to test the validity of our impact parameters. To perform the simulation we took advantage of the iSALE-3D shock physics code (Elbeshausen et al., 2009; Elbeshausen & Wünnemann, 2011), based on the solver described in Hirt et al. (1974). The code includes a strength model (Collins et al., 2004; Melosh et al., 1992; Ivanov et al., 1997) and a porosity compaction model (Wünnemann et al., 2006; Collins et al., 2011) and its development history is described in Elbeshausen et al. (2009).

We used iSALE-3D to simulate the formation of Cornelia crater (Lat: 9.4 S, Lon: 225.6 E), one of the dark craters identified and studied by Reddy et al. (2012). In our simulation the mesh is composed by 400 cells in the horizontal direction, 200 cells in the vertical one and 100 cells in depth, with a spatial resolution of 100 m (including both the impactor and the target layer with some additional space to allow the motion of the excavated material). The impact scenario assumes a spherical dunite impactor with diameter of 1.6 km, porosity of 30% and a final density of 2300 kg/m³ (consistent with a CM-like impactor, Macke et al. 2011) hitting Vesta at 4.75 km/s with an impact angle of 45°. The vestan surface is represented by a basalt layer of about 15 km having density of 2650 kg/m³ (consistent with a howarditic or eucritic layer with about 15% porosity, Consolmagno et al. 2008) and surface gravity of 0.25 m/s². The choice of the composition of the projectile is limited to those materials existing in the simulation package and having proper equation of state. However, as we showed, the density and the porosity of the projectile have been adjusted to better fit a carbonaceous chondrite.

3. Results

As discussed in Sect. 2.1, we run our model over two temporal intervals: the post-Late Heavy

Temporal Interval	Evolving Asteroid Belt	Linear Decay (McCord et al., 2012)	Stationary Asteroid Belt
All Impactors			
3.98 Ga	1141.9	1383.3	1046.4
1.00 Ga	265.3	300.4	262.0
Dark Impactors			
3.98 Ga	244.4	297.1	223.0
1.00 Ga	55.5	64.5	54.8

Table 2: Number of impacts on Vesta due to all impactors and to dark impactors only over the last 3.98 Ga and the last 1 Ga. The column “Evolving Asteroid Belt” reports the values obtained assuming a decaying population in the asteroid belt as in Minton and Malhotra (2010), while the column “Stationary Asteroid Belt” reports those obtained assuming a constant population equal to the present one. The column “Linear Decay” shows the corresponding values obtained using the linear decay approximation adopted by McCord et al. (2012).

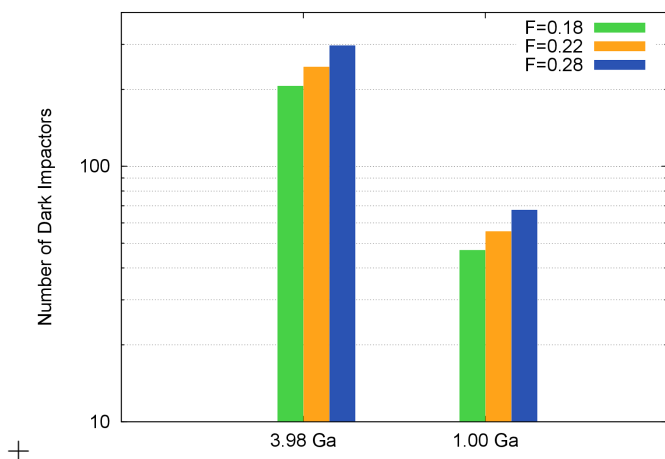


Figure 1: Number of dark impactors on Vesta over the last 3.98 Ga and the last 1 Ga for the different values of the fraction of dark asteroids F_d in the asteroid belt we described in Sect. 2.4.

Bombardment period, i.e. the last 3.98 Ga, and the post-Rheasilvia period, i.e. the last 1 Ga. Before using the model to assess the contamination of Vesta, however, we validated it against the observational features of the dark material on the vestan surface.

3.1. The temporal evolution of the asteroid belt and Vesta’s collisional history

The first comparison we performed was with the number of impacts estimated by McCord et

al. (2012) and the number of impacts that would take place on Vesta if the population of the asteroid belt was stationary at its present level. The results we obtained are summarized in Table 2. As can be seen by comparing the different columns in Table 2, the assumption of a stationary asteroid belt produces results that are closer to those obtained considering a more realistic, exponentially decaying asteroid belt than those obtained assuming a linearly decaying population of asteroids, as instead we did in McCord et al. (2012). The stationary asteroid belt gives a number of impacts that is 10% lower than our reference case of an exponentially decaying asteroid belt, while the linearly decaying asteroid belt results in a number of impacts that is 20% larger than the latter.

We then verified how much the total number of dark impactors is affected by our assumption on the fraction of dark asteroids in the asteroid belt. In Figure 1 we show the number of dark impactors expected on Vesta over the two temporal intervals here considered using the different values for the fraction of dark asteroids we discussed in Sect. 2.4. As can be seen, the number of dark impactors changes by $\pm 20\%$, but the order of magnitude of the results is the same. As a consequence, in the following we will always implicitly refer to our reference case where $F_d = 0.22$.

In Figs. 2 and 3 we show respectively the num-

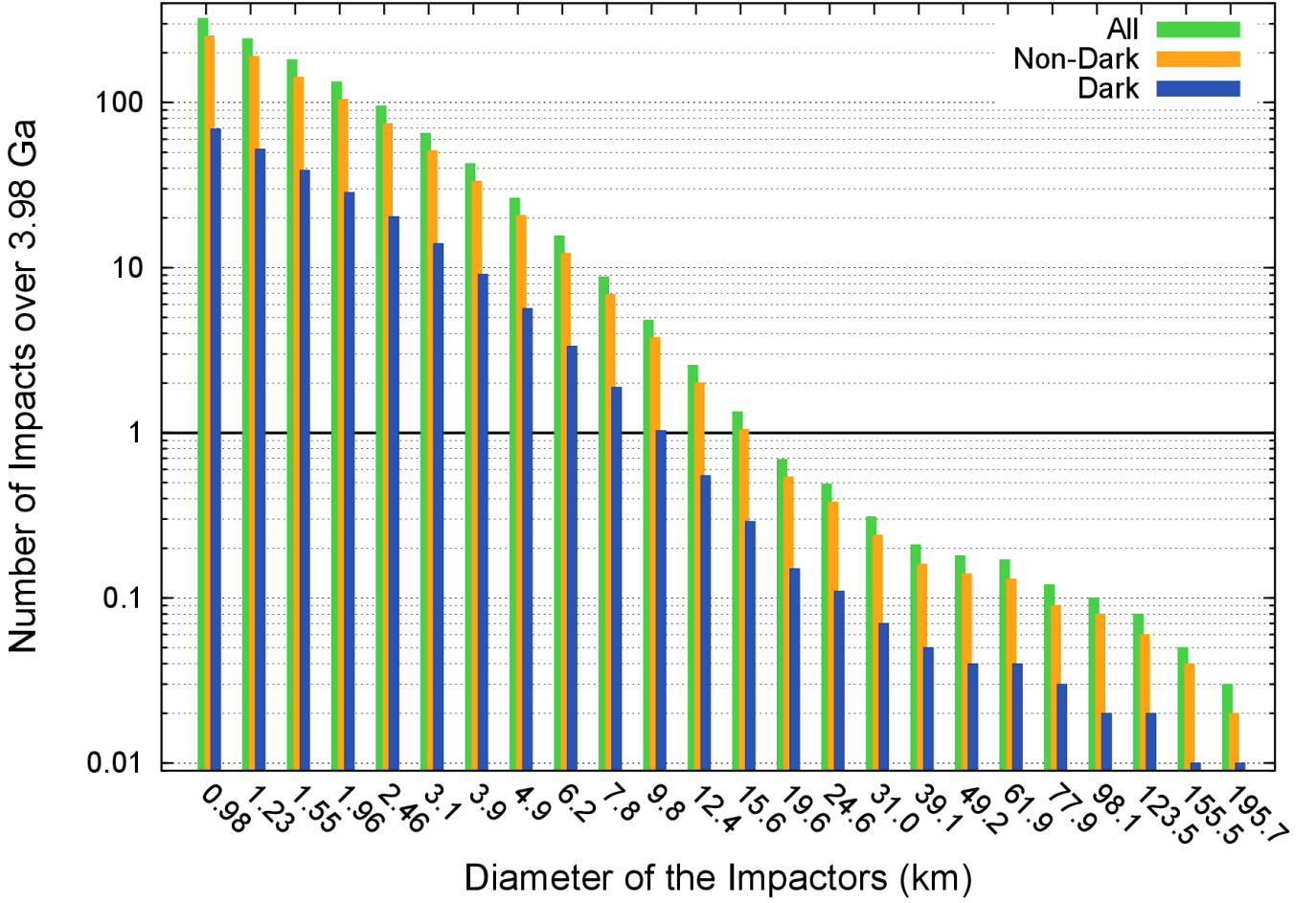


Figure 2: Number of impacts over 3.98 Ga for dark impactors, non-dark impactors and for all impactors for the different size classes from Table 1. We do not account for size classes associated with a number of impacts lower than 1 (i.e. stochastic events) in the assessments of the contamination (see Figure 3).

ber of impacts and the mass delivered by dark, non-dark and by all possible impactors as computed using Eq. 3 for the different size bins from Table 1. In Figure 2 we show only those size bins that are associated with at least a 1% chance of producing one impact over the considered temporal interval. In Figure 3 we show instead only those size bins that are associated with at least 1 impact over the considered timespan.

As over the last 1 Ga the exponentially decaying asteroid belt and the stationary one produce essentially the same results within 1%, in Figs. 2 and 3 we show only the values referring to the last 3.98 Ga. Interested readers can obtain the number of impacts and the mass fluxes of dark and non-dark impactors over the last 1 Ga simply by using the values of Table 1 together with

Eq. 1 (where the factor 1.5 should be dropped as the population of asteroids should be considered stationary) and Eqs. 5 and 6.

3.2. Uncertainties on the number of impacts and on the delivered masses

The uncertainties associated with our estimates of the fluxes of impactors on Vesta are governed by Poisson statistics, therefore $1\sigma = \sqrt{N}$ where N is the population of impactors under consideration. Over the last 3.98 Ga, the 1σ uncertainty on the flux of all possible impactors is of about 3%, while in the case of the dark impactors the 1σ uncertainty is of about 6%. Because of the lower number of events, the 1σ uncertainties on the fluxes of all impactors and of dark impactors over the last 1 Ga become respectively about 6%

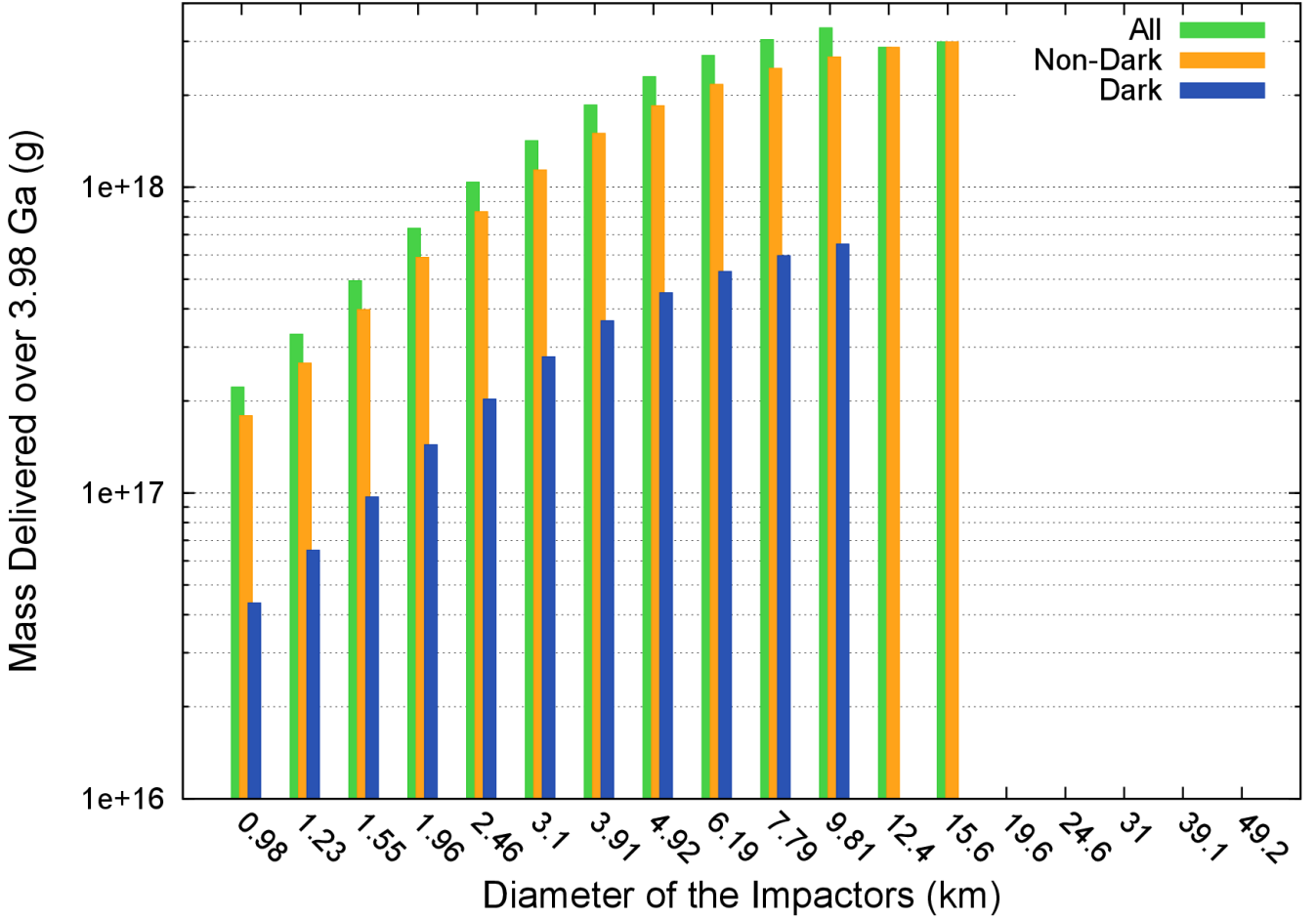


Figure 3: Masses (in g) delivered to Vesta over 3.98 Ga by dark impactors, non-dark impactors and by all impactors. The mass retention efficiency is computed using Eq. 3 so it is the reference retention efficiency we considered in this work. As mentioned in the caption of Figure 2, the delivered masses are computed only for those size classes of impactors that produce at least 1 impact over the considered temporal interval.

and about 13%.

However, a comparison of Figs. 2 and 3 immediately reveals that the delivery of the dark material and, more generally, of all exogenous materials is dominated by the contribution of the largest impactors. In particular, the largest impactors for both dark and non-dark asteroids are associated with a single impact event over the relevant timespan (see e.g. Figure 2). According to Poisson statistics, the uncertainty on these impact events is of the same order as the number of events themselves, i.e. the events may or may not have taken place over the considered temporal interval.

The uncertainty on the single largest dark impactor in Figure 2 translates in a 30% uncertainty

on the total budget of the dark material delivered over the last 3.98 Ga (see Figure 3). Analogously, the uncertainty on the single largest non-dark impactor in Figure 2 implies a 15% uncertainty on the total budget of the exogenous (i.e. dark and non-dark) material delivered over the same timespan (see Figure 3). Over the last 1 Ga, the uncertainties in the number of the largest impactors translate in uncertainties of about 20% on the total delivered masses of dark and non-dark materials.

Even when we consider only a specific set of values for the parameters of the model (e.g. F_d , f_r , etc.), the uncertainties on the numbers of impactors imply that the 1σ errors affecting the delivered amounts of exogenous materials cannot be

smaller than 20 – 30%. As a consequence, when comparing the predictions of our model to the data supplied by the Dawn mission or by the laboratory studies of the HED meteorites, we will limit ourselves to consider only the orders of magnitude of the relevant quantities.

3.3. Dark craters on Vesta and inside Rheasilvia

The Dark Material Deposits catalogue (Palomba et al., 2013, this issue) produced by analysing the data supplied by VIR (De Sanctis et al., 2011, 2012b) has revealed that more than 50% of the occurrences of the dark material are associated with impact-related features (crater rims, crater slopes, crater walls, ejecta). If we look to the global distribution of the dark craters and of the regions characterized by the lowest reflectance values we show in Figure 4 (where we considered the reflectance at $1.4\ \mu\text{m}$ as our proxy), we can see that both the highest density of dark craters and lowest reflectance values are associated with the oldest, highly-cratered terrains of Vesta (Marchi et al., 2012).

This is in agreement with the distribution of the H-rich material mapped by GRaND (Prettyman et al., 2012), with the distribution of the OH mapped by VIR (De Sanctis et al., 2012a) and with the scenario of secular accumulation of the dark material due to a continuous flux of dark impactors. The older (from the cratering point of view) a terrain is, the more dark material will accumulate since the last resetting event. More recent terrains instead had their content of exogenous material reset and had less time to accumulate it again. The ages of the oldest terrains, however, are still not well constrained (Marchi et al., 2012); as a consequence, we cannot use them as a reliable test for our model from the point of view of the expected number of dark features.

The age of the Rheasilvia basin, however, is much better constrained (1 Ga, Marchi et al. 2012; Schenk et al. 2012). The Rheasilvia basin, moreover, represents the optimal test-bed for this kind of comparison, as the extensive excavation (Jutzi et al., 2013) caused by its formation and the formation of the partially underlying Veneneia basin erased all pre-existing deposits of exogenous

material. This basin is therefore a “clean slate” that recorded all impact events due to dark impactors over the last 1 Ga. The first test against the observational data from the Dawn mission that we performed on our model, therefore, was to compare the number of dark impactors hitting Vesta in the last 1 Ga with the number of dark craters observed inside the Rheasilvia basin.

The Rheasilvia basin has a diameter of ~ 500 km (Schenk et al., 2012): a simple back-of-the-envelope calculation shows that its surface accounts for 22.6% of the total surface of Vesta computed from its mean radius $R_V = 262.7$ km. This implies that, statistically, 12.5 ± 3.5 dark impactors should fall inside Rheasilvia in our reference case for the flux of dark projectiles. If we consider all the different values of F_d that we discussed in Sect. 2.4 and Sect. 3.1, we obtain a minimum of 10.6 ± 2 and a maximum of 15.3 ± 4 of dark craters inside Rheasilvia, i.e. a variability of about 20% respect to our reference value. A comparison with Figs. 11 and 12 from Reddy et al. (2012) reveals 12 dark craters inside or overlapping the rim of Rheasilvia. If we consider only the dark craters that Reddy et al. (2012) identified inside the Rheasilvia basin, the total drops to 10 dark craters. Finally, an updated count that we performed in the framework of this study resulted in 16 dark craters inside or on the rim of the Rheasilvia basin. All these values are consistent (generally within 1σ) with the range of possible outcomes resulting from our model, supporting the scenario of a continuous and isotropic flux of dark impactors on Vesta and our choice of parameters.

As a side product of this test of the reliability of our model, we can take advantage of the impact fluxes we computed to estimate the probability of the scenario assumed by Jutzi et al. (2013) for the formation of Veneneia and Rheasilvia. Jutzi et al. (2013) assumed that the two basins formed due to the impact of ~ 60 km wide asteroids, colliding with Vesta with velocities slightly above the average impact velocity computed by O’Brien and Sykes (2011). The probability of Vesta being hit by an asteroid with this diameter over the last 3.98 Ga is $\sim 16\%$. The chances of Vesta being

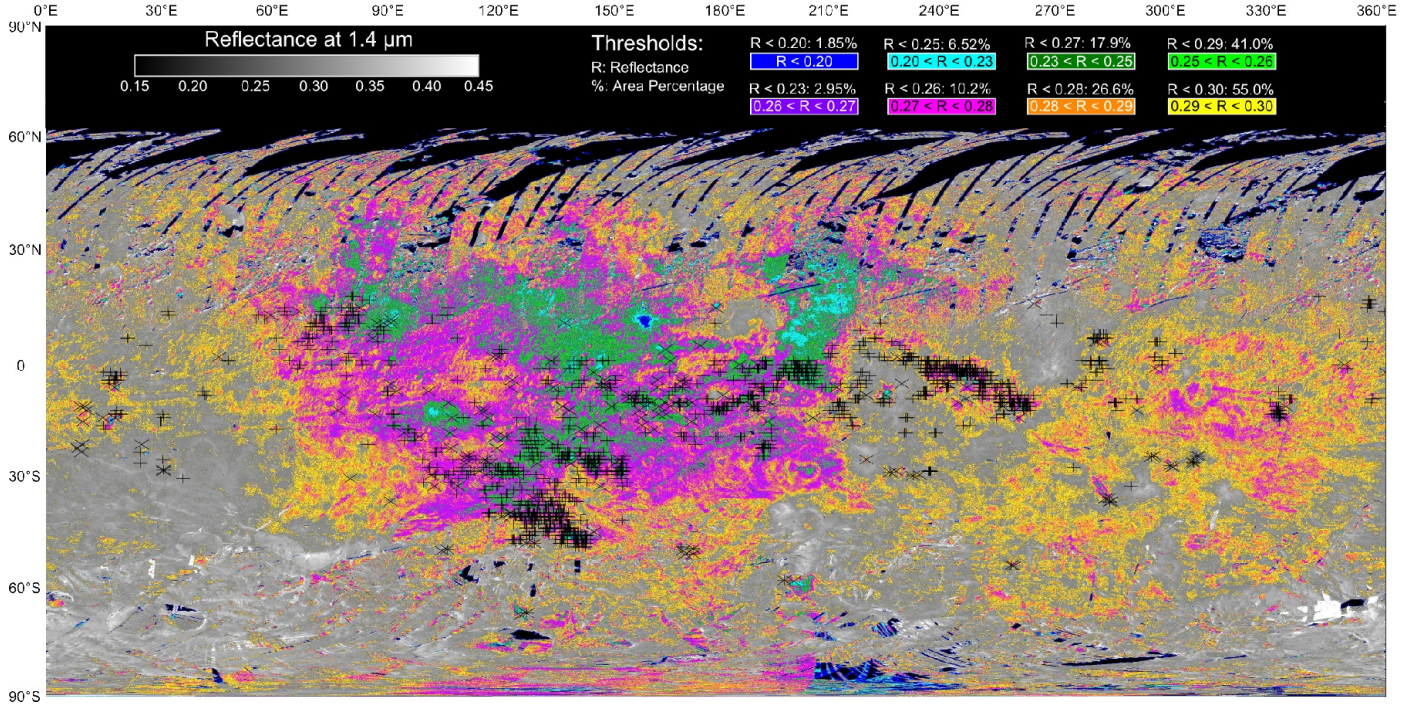


Figure 4: Distribution of the dark material on the surface of Vesta as revealed by the visual and near-infrared spectrometer VIR on-board the Dawn spacecraft using the spectral reflectance at $1.4 \mu\text{m}$ as our proxy. Black symbols indicate the dark craters and the dark spots identified with the color data from the Framing Camera on-board the Dawn spacecraft during the HAMO phase at about 60 m/pixel (Reddy et al., 2012). Also indicated are the area percentages of the surface of Vesta that are associated with the different threshold levels of reflectance we selected.

hit by two such asteroids in the same temporal interval, therefore, are of the order of 2 – 3%. If we require that one of the two impactors is a low albedo asteroid, as proposed by Reddy et al. (2012), the chances of this scenario can drop down to 0.5%. It must be noted, however, that Reddy et al. (2012) assumed that Veneneia was formed by a smaller impactor than the one of Jutzi et al. (2013).

3.4. Cornelia crater as a case study and a calibration test

In their work, Reddy et al. (2012) used the Cornelia crater as a case study to illustrate the spectral behavior and the distribution of the dark material associated with a crater (see Figure 7 in Reddy et al. 2012). To investigate whether the dark material inside Cornelia could have been delivered by a low albedo impactor hitting Vesta with the average impact velocity and angle we assumed in our model, we simulated the formation of Cornelia using the iSALE-3D shock physics code as detailed in Sect. 2.8.

The result of our simulation is presented in Figure 5. The crater resulting from the simulation has a depth of 2.5 km and a diameter of about 11 km, which is comparable to the depth of 3.7 km and the diameter of 12.6 km measured for Cornelia by Vincent et al. (2013). As can be seen in Figure 5, at the end of the simulation the distribution of the projectile’s material inside the crater reproduces reasonably well the bilobate distribution of the dark material, the region devoid of dark material upstream of the crater center and their symmetry respect to the impact direction. The main differences between the results of the simulation and the dark material inside Cornelia are due to a series of subsequent landslides along the crater walls, easily identifiable as a set of mostly circular, brighter regions among the dark material near the top of the crater walls.

A small fraction of the projectile’s material falls outside the rim of the crater downstream of the impact direction, covering an area of about 11.52 km². This is less than what observed by Reddy et

al. (2012), but this difference can be due either to our choice of the physical properties of target and impactor or to the fact that in the specific case of Cornelia the impactor had a higher velocity or a higher (respect to the local vertical) impact angle. The match between the real and the simulated Cornelia craters is nevertheless sufficiently good to confirm our choice of the impact parameters in the model.

3.5. Continuous flux, stochastic events and micrometeoritic flux

As we mentioned in Sect. 3.2, the comparison of Figs. 2 and 3 shows that the delivery of the exogenous materials is dominated by the contribution of the largest impactors. The 1 – 3 largest impact events of each class of impactors (i.e. dark and non-dark) deliver in fact about 30% of the whole budget of the respective exogenous material over 3.98 Ga. If we consider instead the largest $\sim 6 - 8$ impact events, the delivered fraction of the relevant exogenous material increases to about 50%.

The comparison between Figs. 2 and 3 also shows us something else. Extrapolating from the results of Bottke et al. (2005b) for the size-frequency distribution of the asteroid belt at sub-km diameters, the increasing trend in the number of impacts for decreasing diameters of the impactors should continue and Vesta should have received $\sim 10^6$ impacts of decimetre-sized particles over the last 3.98 Ga. According to the results of Gladman et al. (2009), however, the decreasing trend in the mass contribution to the exogenous material for decreasing diameters of the impactors should continue, as a reflection of the differential slope being shallower than -3 as discussed in Sect. 2.1.

These considerations should immediately confirm that the “micrometeoritic flux” and the “stochastic events” hypotheses (Reddy et al., 2012; De Sanctis et al., 2012a) are nothing more than two aspects of the “continuous flux” scenario. Micrometeorites did contribute to the contamination of Vesta over the last ≈ 4 Ga but, as also pointed out by Reddy et al. (2012), their contribution was not the dominant one. The largest impactors, on the other hand, did contribute a sig-

nificant fraction of the dark material. However, to consider only their contribution would underestimate the budget of the exogenous material by a factor 2 – 3 and would not explain the observed number of dark craters on Vesta, especially those inside Rheasilvia.

3.6. Cratering erosion of Vesta and the removal of the exogenous material

Now that our model is reasonably validated for what concerns the choice of the impact parameters and the predictions on the flux of impactors, we can use it to explore the contamination history of Vesta. We will start by assessing how old the dark material on the surface of the asteroid can be and how reasonable our choice of focusing on the post-Late Heavy Bombardment phase is. We will first investigate the role of cratering erosion, while in Sect. 3.7 we will explore that of crater saturation and ejecta blanketing.

The erosion of Vesta over the last 3.98 Ga, estimated using Eq. 13, amounts to about 8.2×10^{19} g (0.03% of the present vestan mass). This is equivalent to the loss of about 30 m of material extending outward from the present surface of the asteroid. Over the last 1 Ga, the mass loss amounts instead to about 1.3×10^{19} g (0.005% of the present vestan mass) or, equivalently, to the erosion of about 5 m of material.

Using Eq. 13 with the sizes of the impactors that Jutzi et al. (2013) assumed to have formed Veneneia and Rheasilvia, we can estimate that the mass loss associated with the two basins would be of the order of 10^{21} g ($\sim 0.4\%$ of the present vestan mass). The erosion of the asteroid is therefore dominated, over the last 4 Ga, by these two impact events. Note, however, that the match between the results obtained by Jutzi et al. (2013) and the compositional signatures of the Rheasilvia basin is still matter of debate (McSween et al., 2013), so the values we provided should be considered only for comparison purposes.

Even ignoring the roles of Veneneia and Rheasilvia, however, the balance between mass loss and mass gain is markedly in favour of the former. If, over a certain temporal interval, impacts were numerous enough to saturate the sur-

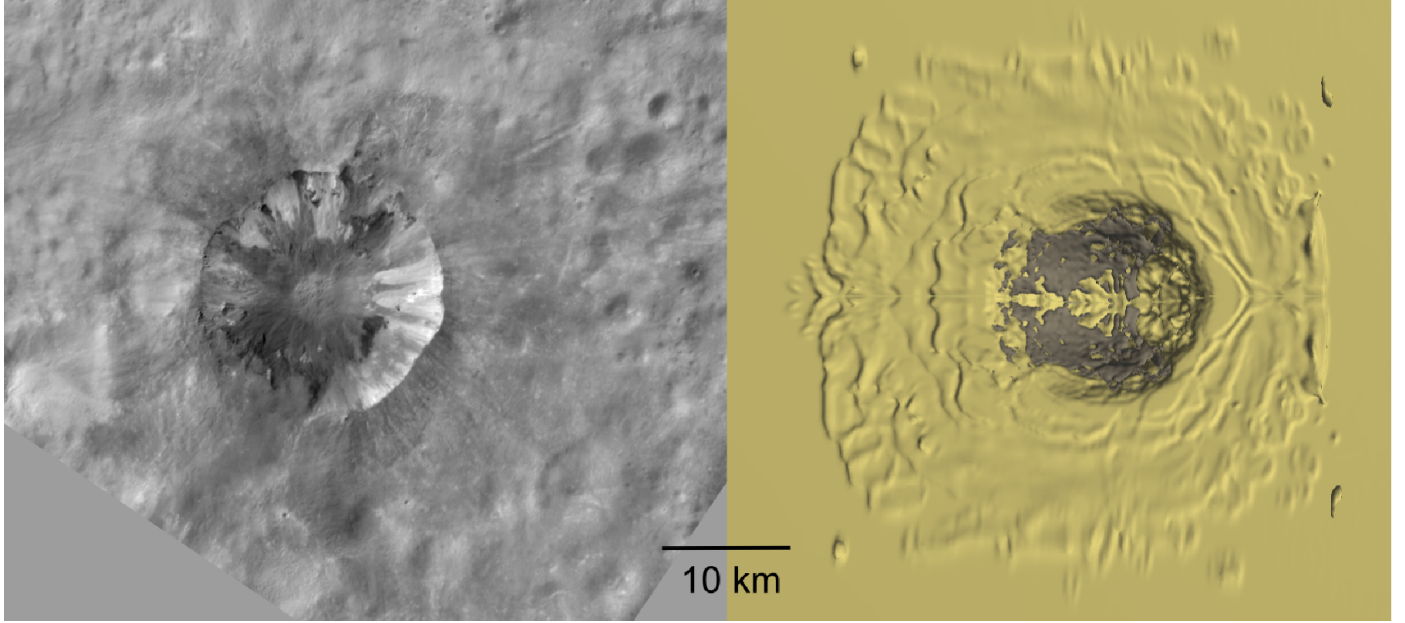


Figure 5: Image of the Cornelia crater taken by the Framing Camera on-board the Dawn spacecraft during the HAMO phase (left panel) and the snapshot of the related hydrocode simulation, showing the distribution of the impactor’s material inside the crater (right panel). The material from the impactor is shown in dark gray color, while the target material is shown in yellow color. The impact direction is from the right and cuts the figure horizontally in the middle. The bilobate distribution of the projectile’s material is symmetrical respect to the impact direction. The simulation also reproduced correctly the region devoid of dark material extending upstream from the crater center and symmetric respect to the impact direction. The main difference between the results of the simulations and the dark material inside Cornelia are due to a series of landslides that are identifiable as a set of mostly circular, brighter regions among the dark material near the top of the crater walls.

face of Vesta (as we will discuss in Sect. 3.7), the erosive effects associated with cratering could have removed a significant fraction of the previously deposited exogenous material.

3.7. Crater saturation and blanketing effects

As we mentioned previously, from the point of view of the observations of the Dawn spacecraft, the blanketing due to the ejecta produced by impacts of non-dark impactors counteracts the deposition of dark material by the dark impactors. Moreover, as we discussed in Sect. 3.6, all impacts contribute to the erosion of the surface of Vesta and, therefore, to the removal of any previously deposited exogenous material.

In Figure 6 we show the crater populations produced by impacts on Vesta over the last 3.98 Ga and the last 1 Ga. In the plot we show also the 5% and 13% saturation levels: these two threshold levels represent respectively the minimum R-value for which a crater population can reach equilib-

rium (Melosh, 1989) and the R-value estimated for Mimas, whose surface is the most densely cratered in the Solar System (Melosh, 1989).

As can be immediately seen, the crater population produced over the last 1 Ga does not cause any saturation effect. The impacts that Vesta received over the last 3.98 Ga, however, can produce saturation levels comprised between 5% and 13%. This result is in agreement with the crater counting of Marchi et al. (2012), where the oldest terrains on Vesta approach the 10% saturation level, and implies that the mass loss due to cratering erosion discussed in Sect. 3.6 globally affected the surface of the asteroid.

The effects of the Late Heavy Bombardment in terms of crater production are equivalent to another 1 Ga of collisional evolution (~ 300 impacts, S. Pirani, Master Thesis at the University of Rome “La Sapienza”; see also Turrini 2013). Once these craters and the two southern basins Rheasilvia and Veneneia are added to those pro-

duced in the following 3.98 Ga, it would appear that the crater record on the surface of Vesta cannot allow us to probe much earlier than the Late Heavy Bombardment itself (as suggested also by Turrini 2013).

Given that impacts remove more material than they deposit, it is therefore likely that the exogenous material delivered to Vesta during its first 0.5 Ga of life was mostly stripped off by later impacts. In this case, the bulk of the dark material we see today on Vesta was brought on the asteroid after the Late Heavy Bombardment, justifying our initial choice of focusing on the post-Late Heavy Bombardment timespan.

Even when the crater production rate becomes low enough not to cause saturation effects, ejecta blanketing can still influence the amount of the dark material that reside on the surface of Vesta by burying it at different depths. We therefore computed the extension globally covered by ejecta over the two temporal intervals we focused on. The results are summarised in Table 3, where we can see that the cumulative amount of ejecta produced over 3.98 Ga would be enough to cover 1.7 times the surface of Vesta. The fact that part of the dark material deposited in the last 3.98 Ga should be buried by later ejecta provides a natural explanation to the dark veneers observed in crater walls by Jaumann et al. (2012). The ejecta produced over the last 1 Ga, on the contrary, would affect only 36% of the vestan surface.

We used our model to estimate what could be the plausible age of the dark material currently visible on the surface of Vesta. Note that here we are referring only to the dark material that is observed by the Framing Camera and the VIR spectrometer on-board the Dawn spacecraft, which are sensitive to the topmost ~ 1 cm of the vestan regolith. The contaminants mixed in the topmost 1 m of the vestan regolith are instead measured by GRaND and will be discussed in Sect. 3.8 and Sect. 3.9. As we showed in Table 3, impacts over the last 2.6 Ga produce enough ejecta to cover a surface equal to that of Vesta. The dark material deposited from 2.6 Ga ago to now should, on average, remain exposed on the surface of the asteroid, confirming the prediction we made in

the Supplementary Information of McCord et al. (2012). The surface coverage due to the dark material younger than 2.6 Ga should be of the order of 14% of the vestan surface.

The values of the surface coverage here estimated should be corrected, however, for the still undetermined effects of the fraction of buried dark material that was exposed by later impacts and of the dark material mixed in the regolith by the micrometeoritic flux. Nevertheless, in terms of orders of magnitude the darkened surface visible to date on Vesta should vary between $\sim 10\%$, which is the same order of magnitude of the darkest regions in Figure 4 ($R < 0.26$ or, equivalently, up to the magenta region), and $\sim 30\%$, which is the same value estimated by GRaND for the extension of the most H-rich (H concentration equal to or higher than $250 \mu\text{g/g}$, Prettyman et al. 2012) regions.

Note that, if we compute the R values of the crater population produced over the last 2.6 Ga and plot the results in the same way as Figure 6, we obtain a saw-like structure where the peaks at 20 km, 40 km and 80 km would be above the 5% saturation level. It is therefore possible that craters produced over the last 2.6 Ga removed part of the dark material already on the surface. This could explain the existence of the dark spots not associated with craters observed on Vesta (Reddy et al., 2012). The relevant craters could have been removed by later impacts leaving only the dark material deposited outside their borders, e.g. in the downstream region respect to the impact direction (Artemieva and Pierazzo, 2011).

3.8. Contamination by dark and water-equivalent materials

Since the previous results provided us a clearer picture of the survival of the dark material exposed on the vestan surface or buried in the vestan regolith, we can now proceed to quantitatively estimate the amounts of dark material and water-equivalent material delivered since the Late Heavy Bombardment and compare them with the measurements supplied by the GRaND instrument on-board the Dawn spacecraft.

Temporal Interval	Non-Dark Blanketing (units of vestan surface)	Dark Blanketing (units of vestan surface)
3.98 Ga	1.70	0.25
2.20 Ga	1.00	0.14
1.00 Ga	0.36	0.04

Table 3: Amounts of the vestan surface affected by the ejecta blanketing due to all impactors (Eq. 11) and darkened by the fragments of the dark impactors (Eq. 12) over the two temporal intervals considered in this work. Also shown is the age (2.6 Ga) for which the blanketed area becomes equal to the surface area of Vesta. The quantities are expressed in units of the surface area of Vesta.

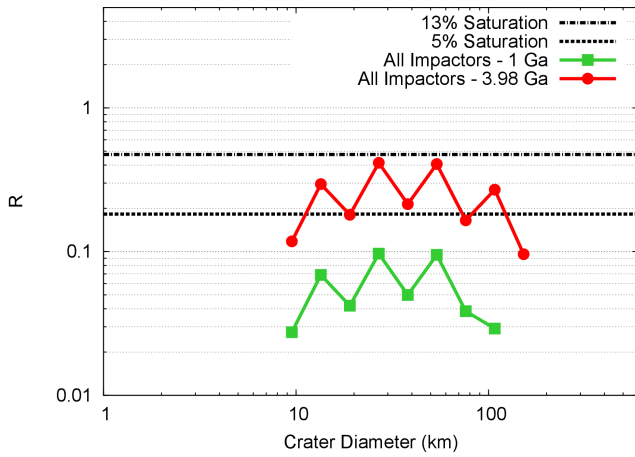


Figure 6: R-plot of the crater population produced on Vesta by all impactors over the last 3.98 Ga and the last 1 Ga. The 5% and 13% saturation levels are shown for reference. Craters with diameter comprised between 20 km and 80 km and between 120 km and 160 km can cause saturation effects on the surface of Vesta over the 3.98 Ga. The effects of Veneneia and Rheasilvia are not included in this plot. The differences between these curves and the similar curve relative to the last 3.5 Ga shown in Turrini (2013) and based on the data from McCord et al. (2012) are mainly due to the different binning.

If we focus only on the size bins from Table 1 that are associated with at least 1 impact event respectively of dark, non-dark and all kind of impactors over the desired timespan (see e.g. Figure 2 for the case of the last 3.98 Ga), we can use the fluxes of impactors we computed to estimate the amount of the different exogenous materials delivered to Vesta (see e.g. Figure 3 for the case of the last 3.98 Ga). In this section we will focus only on the dark material and the associated water-

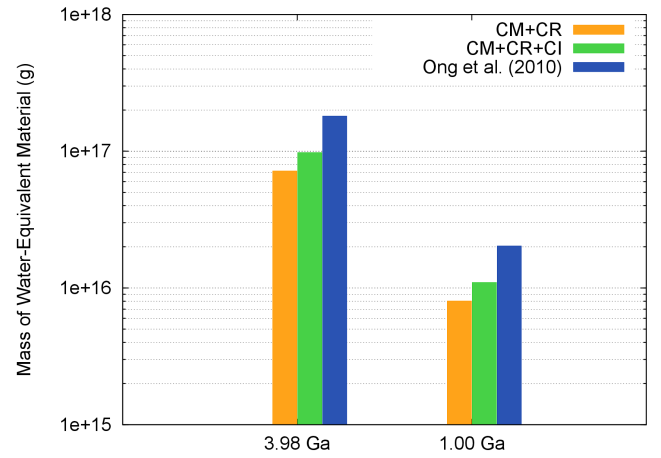


Figure 7: Masses (in g.) of water-equivalent material delivered to Vesta over the last 3.98 Ga and the last 1 Ga by dark impactors for the different values of the fraction of potential water-carriers F_w we described in Sect. 2.4.

equivalent material. We will discuss the cases of Fe and Ni in Sect. 3.9.

As shown in Table 4, over the last 3.98 Ga Vesta would receive between 5.2×10^{17} g and 1.8×10^{18} g of dark material according, respectively, to Eqs. 4 and 3. Over the last 1 Ga, the amount would range between 5.8×10^{16} g and 2.0×10^{17} g again according, respectively, to Eqs. 4 and 3. As the masses computed using Eqs. 3 and 4 always differ by a constant 3.4 factor, in the following we will use the values given by Eq. 3 as our guideline and will discuss the implications of a lower retention efficiency as the one given by Eq. 4 only for the final results.

The delivered amounts of dark material previously discussed would be associated with the de-

livery of about 7.2×10^{16} g of water-equivalent material over the last 3.98 Ga and of about 8.0×10^{15} g over the last 1 Ga, as shown in Table 4. As we show in Figure 7, the inclusion of CI chondrites among the carriers of water-equivalent material to Vesta would result in amounts 1.4 times as large. If instead we consider the water delivery rate assumed by Ong et al. (2010), the amount of water-equivalent material retained by Vesta would be about 2.5–3 times larger than our reference case. In the following, we will focus on our reference case as it supplies the most conservative estimate of the amount of water-equivalent material.

The GRaND detector is sensitive to the composition of the top-most ~ 1 m of the surface of Vesta. The water-equivalent material estimated by GRaND should therefore represent a fraction of the total amount of the water-equivalent material mixed in the vestan regolith. The exact relationship between the value estimated by GRaND and the total amount of water-equivalent material depend on the unknown degree of its mixing in the vestan regolith and its uniformity with depth. From the H measurements of GRaND, Prettyman et al. (2012) estimated a globally-averaged minimum content of 2.7×10^{15} g of equivalent H_2O per meter depth of regolith. The nature of this lower bound, to first order, results in the removal of the post-Rheasilvia contribution of exogenous material.

The lower bound measured by Prettyman et al. (2012) is in agreement with the range of values we reported in Table 4 and in Figure 7. After removing the contribution of the post-Rheasilvia water-equivalent material, our model gives us an amount of water-equivalent material between 6.4×10^{16} g. and 1.9×10^{16} g. This would imply that the water-equivalent material present in the top-most 1 m of the vestan regolith accounts for 4–15% of the total budget of water-equivalent material, i.e. the regolith is not necessarily uniformly mixed but present a gradient of increasing concentrations moving toward the surface.

This is consistent with the global picture obtained by our model once we take into account the results on the ejecta blanketing (see Table 3 and Sect. 3.7). The dark material deposited before 2.6

Ga ago was likely buried at different depths by the ejecta produced by subsequent impacts, thus explaining the veneers of dark material exposed at different depths in the walls of craters (Jaumann et al., 2012). The dark material deposited after 2.6 Ga, on the contrary, likely remained nearer to the surface and was mixed into a more limited amount of regolith by small-scale or micrometeoritic impacts.

When we consider only the contribution of the last 2.6 Ga, the amount of water-equivalent material delivered would range between 3.6×10^{16} g. and 1.1×10^{16} g. Once we subtract the post-Rheasilvia contribution, the presence in the top-most 1 m of regolith of 10–30% of the water-equivalent material delivered between 2.6 Ga ago and 1.0 Ga ago would be enough to explain the measurements of GRaND, leaving us enough margin to account for the removal of exogenous material due to the formation of Veneneia and Rheasilvia (not considered in this model).

3.9. Contamination by Fe and Ni

Based on the agreement between our model and the observations of the Dawn spacecraft for what it concerns the flux of dark impactors and the delivery of water-equivalent material, we used our model to assess the delivery of Fe and Ni on Vesta by impacts and its implications for the composition of the vestan regolith. The results we obtained and that we will now discuss are summarized in Table 4. Over the last 3.98 Ga, Vesta should have received between 1.1×10^{18} g and 3.8×10^{18} g of Fe and between 5.6×10^{16} g and 1.9×10^{17} g of Ni. Over the last 1 Ga, the exogenous Fe should vary between 1.5×10^{17} g and 5.0×10^{17} g and the exogenous Ni between 7.4×10^{15} g and 2.5×10^{16} g.

The Fe content of the vestan regolith has been constrained by the observations of GRaND (Prettyman et al., 2012; Yamashita et al., 2013), which showed that the average value of Fe/O and Fe/Si (Prettyman et al., 2012) and the range of values of Fe mapped by Yamashita et al. (2013) are consistent with the values characteristic of HED meteorites (see Prettyman et al. 2012, Supplementary Information). In particular, the composition

Temporal Interval	Dark Material (g)	H ₂ O (g)	Non-Dark Material (g)	Exogenous Material (g)	Fe (g)	Ni (g)
Svetsov						
3.98 Ga	1.8×10^{18}	7.2×10^{16}	1.7×10^{19}	1.9×10^{19}	3.8×10^{18}	1.9×10^{17}
1.00 Ga	2.0×10^{17}	8.0×10^{15}	2.3×10^{18}	2.5×10^{18}	5.0×10^{17}	2.5×10^{16}
Svetsov-Ong						
3.98 Ga	5.2×10^{17}	2.1×10^{16}	5.1×10^{18}	5.6×10^{18}	1.1×10^{18}	5.6×10^{16}
1.00 Ga	5.8×10^{16}	2.4×10^{15}	6.8×10^{17}	7.4×10^{17}	1.5×10^{17}	7.4×10^{15}

Table 4: Masses of the dark (e.g. carbonaceous chondrites), non-dark (e.g. ordinary chondrites) and both exogenous materials, and masses of water-equivalent material (labelled “H₂O”), Fe and Ni delivered to Vesta over the last 3.98 Ga and 1 Ga using Eq. 3 (label “Svetsov”) and Eq. 4 (label “Svetsov-Ong”) to determine the retention efficiency of the asteroid.

of the vestan surface proved consistent, on the whole, with that of howardites (Prettyman et al., 2012; Yamashita et al., 2013).

To understand the implications of the Fe delivery for the composition of the vestan regolith, we performed the following tests. As our first test, we considered a layer of 100 m of regolith (the minimum thickness according to present estimates) with an average density $\rho_{reg} = 2000 \text{ kg/m}^3$, whose total mass is $1.7 \times 10^{20} \text{ g}$. If we assume that the layer is uniformly mixed and we add to its natural Fe content (assumed to be 13.8 wt% by Yamashita et al. 2013 and in this work) the Fe contribution of all the exogenous material delivered over the last 3.98 Ga (see Table 4), we get maximum Fe contents of 13.9 – 14.3 wt%.

As our second test, we followed our results on the contamination by water-equivalent material and focused only on the topmost 1 m of the regolith, keeping the same density and average Fe content as in our previous test. The resulting mass of this 1 m layer is therefore $1.7 \times 10^{18} \text{ g}$. We computed the possible amounts of Fe delivered to Vesta between 2.6 Ga ago and 1 Ga ago and we assumed that 10 – 30% of this Fe (i.e. the same fractions as the water-equivalent material) was mixed in this regolith layer. The maximum Fe content we obtained this way is 15.7 wt%. The contribution of the following 1 Ga, ignoring the impactors falling inside Rheasilvia as its contami-

nation has been set back to zero by the formation of the basin, would raise the Fe content of the oldest terrains to about 16%.

In the first test, the values we obtain are well inside the range of the measurements performed by GRaND and are within 1σ ($\pm 10\%$, Prettyman et al. 2012) from their average value (Prettyman et al., 2012; Yamashita et al., 2013). In the second test, while our values fall outside the range of the measurements of GRaND (Yamashita et al., 2013), they nevertheless fall inside 2σ from the average Fe content measured by GRaND (Prettyman et al., 2012). Moreover, the variations caused by the exogenous Fe with respect to the ranges of possible native Fe contents of eucrites, diogenites and howardites were limited (Prettyman et al., 2012; Yamashita et al., 2013). Our results are therefore consistent with the observational data and indicate that Fe is not a reliable tracer of the contamination of Vesta.

Differently from the case of Fe, the possibility to investigate the vestan Ni content with GRaND is still under evaluation. As a consequence, at present we can test the results of our model only against the HED meteorites. We did, nevertheless, perform the same tests as for the case of Fe. In the first test, we added the exogenous Ni from Tab 4 to our 100 m thick layer of regolith and obtained an average Ni content varying between $300 \mu\text{g/g}$ (using Eq. 4 for the retention efficiency)

and 1100 $\mu\text{g/g}$ (using Eq. 3 for the retention efficiency). This range is remarkably similar to that covered by the most Ni-rich howardites among the samples of Warren et al. (2009). It is also noteworthy that our range of values is practically identical to that of the samples that Warren et al. (2009) label as “regolithic howardites.” In the second test, if we add the contribution of the exogenous Ni delivered between 2.6 Ga and 1 Ga ago to the native Ni content of the topmost 1 m of regolith, we obtain that the Ni concentration can reach values up to 3600 $\mu\text{g/g}$. Interestingly, the Ni content we obtain this way is of the same order of magnitude as the most Ni-enriched sample of howardites from Warren et al. (2009).

4. Discussion and conclusions

In this work we explored the scenario of a continuous delivery of exogenous material to Vesta due to asteroidal impacts and we investigated its implications for the surface composition. We developed a model for the contamination of Vesta based on the one we originally used in McCord et al. (2012) to estimate the amount of dark material secularly accreted by the asteroid. We took advantage of the observations of the Dawn mission and of the laboratory data on the HED meteorites to verify our model in a quantitative way and, in turn, we used our model to derive possible observations that can help us disentangle the collisional and contamination history of Vesta.

The contamination scenario based on the continuous flux of exogenous material resulting from the secular collisional history of Vesta is one of the three explanations invoked for the dark material (McCord et al., 2012) and the associated OH (De Sanctis et al., 2012a) and H (Prettyman et al., 2012) observed by the Dawn spacecraft. The two alternative explanations propose a dominant role either of the micrometeoritic flux, particularly at the time of the Late Heavy Bombardment, or of stochastic low-velocity impacts with large asteroids. Considering these three explanations as separate mechanisms is however misleading. As we showed with the help of our model, the “micrometeoritic flux” and the “stochastic events” scenar-

ios are actually the end-members of the “continuous flux” scenario.

The present day size-frequency distribution of the asteroid belt implies in fact that sub-km asteroids and micrometeorites represent the bulk of the impactors on Vesta, but their contribution in mass to the contamination is limited (as recognized also by Reddy et al. 2012). Nevertheless, they have an important role in the mixing of the regolith and in determining the distribution of the contaminants with depth, an aspect that needs to be explored in future studies in order to improve the comparison of theoretical prediction with the data supplied by GRaND on the abundances of the different materials in the topmost 1 m of the vestan regolith.

Large impactors, on the contrary, dominate the mass contribution to the contamination of Vesta and the 1 – 3 largest impactors in our model supply about 30% of the total budget of contaminants. The impactors that caused the formation of Rheasilvia and Veneneia, which we did not consider in this work since the scaling laws we used in our model do not necessarily hold for them, could easily have brought more exogenous material than all the other impactors cumulatively. They also likely removed or buried a significant fraction of the previously deposited contaminants, but to date models (see e.g. Jutzi et al. 2013) do not yet reproduce satisfactorily the compositional signatures of the basins they formed (see e.g. McSween et al. 2013 for a discussion). Their role in the erosion and contamination histories of Vesta therefore needs to be further investigated.

Reddy et al. (2012) and De Sanctis et al. (2012a) also proposed that impactors before or across the Late Heavy Bombardment could have supplied a significant, if not the dominant, fraction of the dark material presently observed on Vesta by the Dawn mission. Vesta started collecting significant quantities of exogenous material immediately after the formation of its basaltic crust (see e.g. Turrini et al. 2011; Turrini 2013) but, as soon as the impact velocities in the asteroid belt reached their present values (about 1 Ma after the formation of Jupiter, Turrini et al. 2011, 2012), Vesta started to lose more mass than

the one it accreted (Turrini et al., 2011; Turrini, 2013). Therefore, the accumulation of the exogenous material delivered by the impactors was plausibly counteracted by the cratering erosion they caused.

As we showed with the help of our model, the crater population produced over the last ~ 4 Ga can already produce saturation effects to a level between 5% and 13%, in agreement with the observational data (Marchi et al., 2012). This implies that cratering erosion affected the surface of Vesta to a global scale even after the Late Heavy Bombardment. Once we include the erosion associated with the formation of Rheasilvia and Veneneia to that due to the continuous flux of impactors, it seems likely that most material deposited before and during the Late Heavy Bombardment was removed from the surface of Vesta.

The results of our model highlighted that a full exploration of the link between the collisional and the contamination histories of Vesta over the last 4 Ga is made difficult not only by the possibility of saturation effects among the crater population but also by the blanketing effects associated with crater production. The craters that formed on Vesta over the last 2.6 Ga produced in principle enough ejecta to cover the whole surface of the asteroid. Over the same temporal interval, moreover, the impacts that formed Rheasilvia and Veneneia possibly caused a global blanketing by themselves (Jutzi et al., 2013). These blanketing events make it difficult to assess the number of dark impactors that actually impacted Vesta before the formation of Rheasilvia. The effects of crater saturation and ejecta blanketing, on the other hand, explain in a natural way the dark spots not associated with specific craters (Reddy et al., 2012) and the veneers of dark material exposed on crater walls (Jaumann et al., 2012).

While the ages of the oldest terrains on Vesta are still uncertain (Marchi et al., 2012), the age of Rheasilvia basin is reasonably well constrained to about 1 Ga (Marchi et al., 2012; Schenk et al., 2012). Such a young age implies that saturation and blanketing effects should not have affected the crater population that formed in its interior, therefore making it the best case study to cali-

brate our model. The fraction of dark asteroids in the asteroid belt is still quite uncertain and, to a lower extent, so is the number of dark features inside Rheasilvia. An updated count performed in the framework of this study revealed 16 dark craters instead of the 12 reported by Reddy et al. (2012). Still, in the limits of these uncertainties, all the abundances of dark asteroids that we considered in our model produced the correct order of magnitude of the dark craters observed in Rheasilvia, suggesting that dark asteroids represented about 20 – 30% of the impactors on Vesta (at least during the last 1 Ga).

The second calibration test that we performed focused on verifying whether the average impact velocity and impact angle we assumed for all impactors were appropriate to discuss the delivery of the dark material. We therefore simulated the formation of Cornelia crater and the distribution of the dark material associated with its interior (Reddy et al., 2012) using the iSALE-3D hydrocode. The results of our simulation reproduced reasonably well the bilobate distribution of the dark material inside the crater, the region devoid of dark material upstream to the crater center and their symmetry respect to the impact direction. The main differences between the results of the simulation and the dark material inside Cornelia are due to a series of landslides along the crater walls and near the top of the rim.

As both previous tests produced a reasonable agreement with the observational data, we used our model to estimate the fraction of the vestan surface that should be affected by the dark material and the amounts of the different contaminants brought to Vesta since the Late Heavy Bombardment. Concerning the darkening of the surface of Vesta, the comparison between the darkened area assessed from the Dawn’s observations and the one estimated through our model produces a reasonable match in terms of orders of magnitude. Concerning instead the contaminants, we focused on three tracers: water-equivalent material (i.e. the amount of water needed to explain the observed OH and H on Vesta), Fe and Ni. For the first, the measurements of GRaND provided the distribution and a lower bound to the global abun-

dance of the pre-Rheasilvia water-equivalent material. GRaND also provided the average global Fe content (Prettyman et al., 2012) and its regional distribution (Yamashita et al., 2013) in the vestan regolith, both consistent with the range of values characteristic of HED meteorites. The possibility of detecting Ni with GRaND, instead, is still under assessment, so our results can provide a guideline for future studies.

The amounts of water-equivalent material resulting from our model are consistent with the measurements of GRaND if about 5 – 10% of the water-equivalent material delivered from the Late Heavy Bombardment to the formation of Rheasilvia remained mixed into the topmost 1 m of the vestan regolith. When we focused only on the water-equivalent material delivered after the cumulative effects of ejecta blanketing became less important (i.e. from 2.6 Ga ago to 1 Ga ago), we noticed that the presence of about 10% of the globally delivered water-equivalent material in the topmost 1 m would be enough to match the measurements of GRaND. Once we consider the range of possible depths reached by the vestan regolith (Jaumann et al., 2012), these results suggest that the dark material and the associated water-equivalent material should be present in decreasing quantities with depth, and a significant fraction should have remained in close proximity with the surface.

We took advantage of these results in our assessment of the implications of the delivery of exogenous Fe for the vestan regolith and we considered two scenarios. The first scenario assumed a uniform mixing of the exogenous Fe into a regolith layer whose thickness was set to the minimum value currently estimated through Dawn’s observations (Jaumann et al., 2012). The second scenario assumed instead that the distribution of Fe followed that of the water-equivalent material and resulted in a higher concentration in the topmost 1 m of the vestan regolith. In both cases the effects of exogenous Fe for the total Fe abundance fell inside the range of the GRaND’s uncertainty on the measurements and were globally negligible with respect to the intrinsic variability of the Fe content of HED meteorites. As a consequence, Fe

did not prove to be a reliable tracer of the contamination by exogenous material.

Ni, on the contrary, proved to be an efficient tracer of the contamination: the amounts of Ni estimated to have been delivered by impactors over the last ~ 4 Ga, if mixed uniformly into 100 m of vestan regolith, would produce the range of values observed in those howardites that Warren et al. (2009) label as “regolithic howardites”. If, once again, we take advantage of the results obtained for the water-equivalent material and assume that 10% of the exogenous Ni delivered since 2.6 Ga ago is confined in the topmost 1 m of the vestan regolith, we obtain the Ni content of the most Ni-enriched sample studied by Warren et al. (2009). As a consequence, should GRaND prove capable of detecting Ni in the vestan surface, the study of the Ni abundance and distribution could potentially be a powerful counterpart to dark and water-equivalent materials in unveiling the contamination history of Vesta.

As we pointed out, the model we developed is affected by two intrinsic sources of uncertainties. The first one is our limited knowledge of the real values of the parameters (e.g. the fraction of dark impactors in the asteroid belt) the model uses to characterize the collisional and contamination histories of Vesta. The second one is due to the statistic nature of the evaluation of the collisional history. The largest impact events associated with the estimated fluxes of dark and non-dark impactors, due to their stochastic nature, may or may not have taken place. As these events can contribute 20 – 30% of the budget of the relevant exogenous material, they significantly affect our estimates of the vestan contamination.

This second source of uncertainty can be circumvented in future investigations by calibrating the model over different temporal intervals (hence fluxes of impactors). This can be done by applying the model to selected areas of the vestan surface characterized by different ages and for which the crater records are well preserved. It must be noted that the improvement of the crater catalogue of Vesta, with its extension to the northern hemisphere and the identification of possible ancient degraded craters, will automatically provide

more stringent constraints to the fluxes and the sizes of the impactors. Nevertheless, the model is already capable of reproducing the correct orders of magnitude of the observational and laboratory data available on Vesta and the HED meteorites.

The first source of uncertainty, however, is more difficult to overcome and has important implications, in particular for what concerns the fraction of dark asteroids in the asteroid belt. The calibration we performed on Rheasilvia seems to suggest that the fraction of dark impactors on Vesta over the last 1 Ga ranged between 15 – 30%, in agreement with the estimated abundance of dark impactors done by De Sanctis et al. (2012a). The amount of water-equivalent material estimated using this fraction of dark impactors agrees with the lower bound estimated by GRaND. However, in such a scenario about 70 – 85% of the impactors on Vesta would be non-dark. The present collection of HED meteorites points instead in the opposite direction. Howardites and polymict eucrites have been shown to contain clasts of chondrules, metals, ordinary chondrites, enstatite chondrites and possibly achondrites (Lorenz et al., 2007) but the largest fraction (about 99%, Lorenz et al. 2007) of the xenoliths in HED meteorites is due to carbonaceous chondrites (Zolensky et al., 1996; Lorenz et al., 2007). Presently, we cannot provide a conclusive answer to this conundrum, but we can however formulate some hypotheses on its possible causes.

The first, obvious possibility is that the fraction of dark impactors we are using is not the correct one. Interestingly enough, this has no implications for the amount of delivered Fe and Ni as, to first order, carbonaceous chondrites and ordinary chondrites contain the same fractions of these elements (Jarosewich, 1990). The amount of water-equivalent material would instead increase together with the number of dark impactors. As GRaND provided a lower limit to the H abundance in the topmost 1 m of the vestan regolith, increasing the delivered amount of water-equivalent material does not change the agreement between the model and the observational data. The only difference respect to our original discussion is that the water-equivalent material

does not need to be more concentrated toward the surface but can be more uniformly mixed into the vestan regolith.

The major implication of a larger fraction of dark impactors would be for the number of dark craters, especially those inside Rheasilvia. Increasing the fraction of dark impactors to 90% of the total flux (i.e. about the same fraction of the carbonaceous clasts among the xenoliths in HED meteorites) would produce about 54 ± 7 dark craters inside the basin. The most updated count of the dark craters inside the basin is 16, which is more than 3σ away from the estimated value. On the other hand, such a high frequency of dark impactors would deliver enough dark material and water-equivalent material to reproduce the measurements of the Dawn mission also in the case Veneneia and Rheasilvia globally covered the surface of Vesta with their ejecta blankets, burying most of the oldest contaminants to depths beyond the capabilities of the instruments on-board the Dawn spacecraft.

The second possibility is that the story the HED meteorites tell us about their contamination is not complete or is misleading. It is possible that the collection of samples that fell on the Earth is not representative of the whole surface of Vesta, being linked to one or a few specific cratering events (e.g. Rheasilvia, Veneneia or both). It is also possible that most HED meteorites are actually fragments of V-type asteroids, whose lower gravity respect to the vestan one would make it easier to excavate them. V-type asteroids mainly (but not exclusively, see e.g. McSween et al. 2011, O’Brien and Sykes 2011 and references therein) originated from Vesta, but their small sizes imply that their collisional histories are dominated by sub-km and plausibly sub-m sized impactors, contrary to the case of Vesta discussed in this work. Given that carbonaceous chondrites are composed by more fragile materials than ordinary chondrites (see e.g. Lorenz et al. 2007), it is not implausible that their parent bodies are more easily fragmented or eroded (Lorenz et al., 2007) and that, as a consequence, carbonaceous chondrites represent the bulk of sub-km and micrometeoritic impactors on Vesta and the V-type asteroids. The

dominant presence of carbonaceous chondrites in HED meteorites could therefore be due to a selection effect caused by the smaller sizes of the V-type asteroids.

It is finally possible that, while our samples are indeed representative of Vesta alone, it is our understanding of the data that is not complete. The gravity of Vesta is strong enough that the average retention efficiency does not change dramatically across the range of plausible impact velocities, going from 42% to 68% between 2 km/s and 10 km/s. Therefore, a large fraction of material from the impactors should remain on the surface of Vesta almost independently of the impact velocity. Low impact velocities are generally invoked for the delivery of most of the dark material to explain its preserved hydrated state (Reddy et al., 2012). The less abundant dehydrated clasts in HED meteorites are generally regarded as the product of impacts occurring at higher velocities (Reddy et al., 2012). As pointed out by Lorenz et al. (2007), however, in HED breccias much of the chondritic material is contained in disseminated form. These authors argue that concentration of siderophile elements is significantly larger (sometimes by orders of magnitude) than that associated with the presence of clasts and impact melts, with the bulk of the siderophile elements present as sub-microscopic inclusions. Dark impactors could have therefore hit Vesta over the whole range of impact velocities, supplying contaminants in different form.

Ordinary chondrites are generally less fragile than carbonaceous ones, as showed by the fact that they survive more easily to the passage through the atmosphere of the Earth (see e.g. Lorenz et al. 2007). It is therefore likely that they are better preserved during the impacts on Vesta, and it is conceivable that most of the mass of low-velocity, ordinary chondrite-like (i.e. non-dark) impactors could end up in boulders and fragments larger than those produced by carbonaceous chondrite-like impactors. These larger fragments could be less easily incorporated into the regolith, differently from the smaller fragments produced by faster or more fragile impactors. Most

non-dark contaminants could therefore be present among the vestan regolith as discreet units (large rocks or boulder) instead of being diluted in the form of small fragments and clasts. This scenario would allow to fit the results of our model into all available observational and laboratory constraints, but dedicated, high-resolution impact simulations are needed to test whether this is a viable possibility or not.

Acknowledgements

The authors wish to thank the NASA Dawn project and the entire Dawn team for the development, cruise, orbital insertion, and operations of the Dawn spacecraft at Vesta, and in particular the VIR, GRaND and FC instrument teams on whose data this work is based. The authors gratefully acknowledge the developers of iSALE-3D, including Dirk Elbeshausen, Kai Wünnemann and Gareth Collins, and wish to thank David W. Mittlefehldt for his comments and the discussions that helped to improve the model, Sharon Uy for her assistance in the preparation of the manuscript, and the two reviewers for their comments that contributed to improve both the model and the manuscript. This research has been supported by the Italian Space Agency (ASI) through the ASI-INAF contract I/010/10/0 and by the International Space Science Institute in Bern through the International Teams 2012 project “Vesta, the key to the origins of the Solar System” (www.issibern.ch/teams/originsolsys). The computational resources used in this research have been supplied by INAF-IAPS through the project “HPP - High Performance Planetology.”

References

- Artemieva, N., Pierazzo, E. 2011. The Canyon Diablo impact event: 2. Projectile fate and target melting upon impact. *Meteoritics and Planetary Science* 46, 805-829.
- Bottke, W. F., Nolan, M. C., Greenberg, R., Kolvoord, R. A. 1994. Velocity distributions among colliding asteroids. *Icarus* 107, 255-268.
- Bottke, W. F., Durda, D. D., Nesvorný, D., Jedicke, R., Morbidelli, A., Vokrouhlický, D., Levison, H. 2005. The fossilized size distribution of the main asteroid belt. *Icarus* 175, 111-140.

- Bottke, W. F., Durda, D. D., Nesvorný, D., Jedicke, R., Morbidelli, A., Vokrouhlický, D., Levison, H. F. 2005. Linking the collisional history of the main asteroid belt to its dynamical excitation and depletion. *Icarus* 179, 63-94.
- Bottke, W. F., Vokrouhlický, D., Minton, D., Nesvorný, D., Morbidelli, A., Brasser, R., Simonson, B., Levison, H. F. 2012. An Archaean heavy bombardment from a destabilized extension of the asteroid belt. *Nature* 485, 78-81.
- Britt, D. T., Yeomans, D., Housen, K., Consolmagno, G. 2002. Asteroid Density, Porosity, and Structure. *Asteroids III* 485-500.
- Carry, B. 2012. Density of asteroids. *Planetary and Space Science* 73, 98-118.
- Collins, G. S., Melosh, H. J., and Ivanov, B. A. 2004. Modeling damage and deformation in impact simulations. *Meteoritics and Planetary Science*, 39, 217-231.
- Collins, G., Melosh, H. and Wnnemann, K. 2011. Improvements to the epsilon-alpha porous compaction model for simulating impacts into high-porosity solar system objects. *Int. International Journal of Impact Engineering*, 38, 434-439.
- Consolmagno, G., Britt, D., Macke, R. 2008. The significance of meteorite density and porosity. *Chemie der Erde / Geochemistry* 68, 1-29.
- Coradini, A., Turrini, D., Federico, C., Magni, G. 2011. Vesta and Ceres: Crossing the History of the Solar System. *Space Science Reviews* 163, 25-40.
- Crater Analysis Techniques Working Group 1978. Standard Techniques for Presentation and Analysis of Crater Size-Frequency Data. NASA Technical Memorandum Series.
- Davis, D. R., Chapman, C. R., Greenberg, R., Weidenschilling, S. J., Harris, A. W. 1979. Collisional evolution of asteroids - Populations, rotations, and velocities. *Asteroids* 528-557.
- De Sanctis, M. C., and 11 colleagues 2011. The VIR Spectrometer. *Space Science Reviews* 163, 329-369.
- De Sanctis, M. C., and 20 colleagues 2012. Detection of Widespread Hydrated Materials on Vesta by the VIR Imaging Spectrometer on board the Dawn Mission. *The Astrophysical Journal* 758, L36.
- De Sanctis, M. C., and 22 colleagues 2012. Spectroscopic Characterization of Mineralogy and Its Diversity Across Vesta. *Science* 336, 697.
- Elbeshausen, D., Wünnemann, K., Collins, G. S. 2009. Scaling of oblique impacts in frictional targets: Implications for crater size and formation mechanisms. *Icarus* 204, 716-731.
- Elbeshausen D., Wünnemann K. 2011. iSALE-3D: A three-dimensional, multi-material, multi-rheology hydrocode and its applications to large-scale geodynamic processes. In: *Proceedings of 11th Hypervelocity Impact Symposium (HVIS)*, Fraunhofer Verlag.
- Formisano, M., Federico, C., Turrini, D., Coradini, A., Paccioni, F., De Sanctis, M. C., Pauselli, C. 2013. The heating history of Vesta and the onset of differentiation. *Meteoritics and Planetary Science*, in press. DOI: 10.1111/maps.12134.
- Gladman, B. J., and 11 colleagues 2009. On the asteroid belt's orbital and size distribution. *Icarus* 202, 104-118.
- Gomes R., Levison H.F., Tsiganis K., Morbidelli A. 2005. Origin of the cataclysmic Late Heavy Bombardment period of the terrestrial planets. *Nature* 435, 466-469.
- Hirt, C.W., Amsden, A.A. and Cook, J.L. 1974. An arbitrary Lagrangian-Eulerian computing method for all flow speeds. *Journal of Computational Physics*, 14, pp. 227-253.
- Holsapple, K. A., Housen, K. R. 2007. A crater and its ejecta: An interpretation of Deep Impact. *Icarus* 187, 345-356.
- Holsapple, K. A. 1993. The scaling of impact processes in planetary sciences. *Annual Review of Earth and Planetary Sciences* 21, 333-373.
- Ivanov, B. A., Deniem, D., and Neukum, G. 1997. Implementation of dynamic strength models into 2D hydrocodes: Applications for atmospheric breakup and impact cratering. *International Journal of Impact Engineering*, 20, 411-430.
- Ivanov, B. A., Melosh, H. J. 2013. Two-dimensional numerical modeling of the Rheasilvia impact formation. *Journal of Geophysical Research (Planets)* 118, 1545-1557.
- Jutzi, M., Asphaug, E., Gillet, P., Barrat, J.-A., Benz, W. 2013. The structure of the asteroid 4 Vesta as revealed by models of planet-scale collisions. *Nature* 494, 207-210.
- Jarosewich, E. 1990. Chemical analyses of meteorites - A compilation of stony and iron meteorite analyses. *Meteoritics* 25, 323-337.
- Jaumann, R., and 42 colleagues 2012. Vesta's Shape and Morphology. *Science* 336, 687.
- Jedicke, R., Larsen, J., Spahr, T. 2002. Observational Selection Effects in Asteroid Surveys. In: *Asteroids III*, Eds. Bottke W.F., Cellino A., Paolicchi P., Binzel R., University of Arizona Press, Tucson, pp. 71-87.
- Jutzi, M., Asphaug, E., Gillet, P., Barrat, J.-A., Benz, W. 2013. The structure of the asteroid 4 Vesta as revealed by models of planet-scale collisions. *Nature* 494, 207-210.
- Levison, H. F., Morbidelli, A., Tsiganis, K., Nesvorný, D., Gomes, R. 2011. Late Orbital Instabilities in the Outer Planets Induced by Interaction with a Self-gravitating Planetesimal Disk. *The Astronomical Journal* 142, 152.
- Lorenz, K. A., Nazarov, M. A., Kurat, G., Brandstaetter, F., Ntaflos, Th., 2007. Foreign Meteoritic Material of Howardites and Polymict Eucrites. *Petrology*, 15, 109-125.
- Macke, R. J., Consolmagno, G. J., Britt, D. T. 2011. Density, porosity, and magnetic susceptibility of carbonaceous chondrites. *Meteoritics and Planetary Science* 46,

- 1842-1862.
- Marchi, S., and 11 colleagues 2012. The Violent Collisional History of Asteroid 4 Vesta. *Science* 336, 690.
- McCord, T. B., and 28 colleagues 2012. Dark material on Vesta from the infall of carbonaceous volatile-rich material. *Nature* 491, 83-86.
- McSween, H. Y., Mittlefehldt, D. W., Beck, A. W., Mayne, R. G., McCoy, T. J. 2011. HED Meteorites and Their Relationship to the Geology of Vesta and the Dawn Mission. *Space Science Reviews* 163, 141-174.
- McSween H. Y., and 21 colleagues 2013. Composition of the Rheasilvia basin, a window into Vesta's interior. *Journal of Geophysical Research: Planets* 118, 335346, doi:10.1002/jgre.20057.
- Melosh, H. J. 1989. Impact cratering: A geologic process. Research supported by NASA. New York, Oxford University Press (Oxford Monographs on Geology and Geophysics, No. 11), 1989, 253 p. .
- Melosh, H. J., Ryan, E. V., and Asphaug, E. 1992. Dynamic fragmentation in impacts: Hydrocode simulation of laboratory impacts. *J. Geophys. Res.*, 97, 14735-14759.
- Minton, D. A., Malhotra, R. 2009. A record of planet migration in the main asteroid belt. *Nature* 457, 1109-1111.
- Minton, D. A., Malhotra, R. 2010. Dynamical erosion of the asteroid belt and implications for large impacts in the inner Solar System. *Icarus* 207, 744-757.
- O'Brien, D. P., Morbidelli, A., Bottke, W. F. 2007. The primordial excitation and clearing of the asteroid belt – Revisited. *Icarus* 191, 434-452.
- O'Brien, D. P., Sykes, M. V. 2011. The Origin and Evolution of the Asteroid Belt - Implications for Vesta and Ceres. *Space Science Reviews* 163, 41-61.
- Ong, L., Asphaug, E. I., Korycansky, D., Coker, R. F. 2010. Volatile retention from cometary impacts on the Moon. *Icarus* 207, 578-589.
- Prettyman T. H. 2007. Remote chemical sensing using nuclear spectroscopy. In *Encyclopedia of the solar system*, 2nd edition, Eds. L.-A. McFadden, P. R. Weissman, and T. V. Johnson, pp. 765-786. Academic Press, San Diego, CA.
- Prettyman, T. H., and 19 colleagues 2012. Elemental Mapping by Dawn Reveals Exogenic H in Vesta's Regolith. *Science* 338, 242-246.
- Reddy, V., and 24 colleagues 2012. Delivery of dark material to Vesta via carbonaceous chondritic impacts. *Icarus* 221, 544-559.
- Robert, F. 2003. The D/H Ratio in Chondrites. *Space Science Reviews* 106, 87-101.
- Russell, C. T., and 27 colleagues 2012. Dawn at Vesta: Testing the Protoplanetary Paradigm. *Science* 336, 684.
- Russell, C. T., and 23 colleagues 2013. Dawn completes its mission at 4 Vesta. *Meteoritics and Planetary Science*. DOI: 10.1111/maps.12091.
- Schenk, P., and 13 colleagues 2012. The Geologically Recent Giant Impact Basins at Vesta's South Pole. *Science* 336, 694.
- Svetsov, V. 2011. Cratering erosion of planetary embryos. *Icarus* 214, 316-326.
- Turrini, D., Magni, G., Coradini, A. 2011. Probing the history of Solar system through the cratering records on Vesta and Ceres. *Monthly Notices of the Royal Astronomical Society* 413, 2439-2466.
- Turrini, D., Coradini, A., Magni, G. 2012. Jovian Early Bombardment: Planetesimal Erosion in the Inner Asteroid Belt. *The Astrophysical Journal* 750, 8.
- Turrini, D. 2013. The primordial collisional history of Vesta: crater saturation, surface evolution and survival of the basaltic crust. *Planetary and Space Science*, in press. DOI: 10.1016/j.pss.2013.09.006.
- Vincent, J.-B., Schenk, P., Nathues, A., Sierks, H., Hoffmann, M., Gaskell, R. W., Marchi, S., O'Brien, D. P., Sykes, M., Russell, C. T., Fulchignoni, M., Keller, H. U., Raymond, C., Palmer, E., Preusker, F., 2013. Crater Depth-to-Diameter Distribution and Surface Properties of (4) Vesta. *Planetary and Space Science*, in press. DOI: 10.1016/j.pss.2013.09.003.
- Warren, P. H., Kallemeyn, G. W., Huber, H., Ulf-Møller, F., Choe, W. 2009. Siderophile and other geochemical constraints on mixing relationships among HED-meteoritic breccias. *Geochimica et Cosmochimica Acta* 73, 5918-5943.
- Wünnemann, K., Collins, G., and Melosh, H. 2006. A strain-based porosity model for use in hydrocode simulations of impacts and implications for transient crater growth in porous targets. *Icarus*, 180, 514-527.
- Yamashita, N., T. H. Prettyman, D. W. Mittlefehldt, M. J. Toplis, T. J. McCoy, A. W. Beck, R. C. Reedy, W. C. Feldman, D. J. Lawrence, P. N. Peplowski, O. Forni, H. Mizzon, C. A. Raymond, and C. T. Russell 2013. Distribution of Iron on Vesta. *Meteoritics & Planetary Science*. DOI: 10.1111/maps.12139.
- Zolensky, M. E., Weisberg, M. K., Buchanan, P. C., Mittlefehldt, D. W. 1996. Mineralogy of carbonaceous chondrite clasts in HED achondrites and the Moon. *Meteoritics and Planetary Science* 31, 518-537.